TRN : IN9300655

INDC(IND)-045/G

BARC/1993/E/005

BARC/1993/E/005

सत्यमेव जयते

PROGRESS REPORT ON NUCLEAR DATA ACTIVITIES IN INDIA FOR THE PERIOD JULY 1990 TO JUNE 1992

Compiled by
P. D. Krishnani
Theoretical Physics Division

1993

BARC/1993/E/005

BARC/1993/E/005

GOVERNMENT OF INDIA
ATOMIC ENERGY COMMISSION

PROGRESS REPORT ON NUCLEAR DATA ACTIVITIES IN INDIA FOR THE PERIOD JULY 1990 TO JUNE 1992

Compiled by

P.D. Krishnani
Theoretical Physics Division

BHABHA ATOMIC RESEARCH CENTRE
BOMBAY, INDIA
1993

BIBLIOGRAPHY DESCRIPTION SHEET FOR TECHNICAL REPORT

(as per IS : 9400 - 1980)

01	Security classication :	Unclassified
02	Distribution :	External
03	Report status :	New
04	Series :	BARC External
05	Report type :	Technical Report
06	Report No. :	BARC/1993/E/005
07	Part No. or Volume No. :	
08	Contract No. :	
10	Title and subtitle :	Progress report on nuclear data activities in India for the period July 1990 to June 1992
11	Collation :	75 p., figs., tabs.
13	Project No. :	
20	Personal author (s) :	P.D. Krishnani (comp.)
21	Affiliation of author (s) :	Theoretical Physics Division, Bhabha Atomic Research Centre, Bombay
22	Corporate author(s) :	Bhabha Atomic Research Centre, Bombay - 400 085
23	Originating unit :	Theoretical Physics Division, BARC, Bombay
24	Sponsor(s) Name :	Department of Atomic Energy
	Type :	Government
30	Date of submission :	March 1993
31	Publication/Issue date	March 1993

contd...(ii)

40	Publisher/Distributor :	Head, Library and Information Division, Bhabha Atomic Research Centre, Bombay
42	Form of distribution :	Hard Copy
50	Language of text :	English
51	Language of summary :	English
52	No. of references :	refs.
53	Given data on :	nuclear reaction cross sections

60 Abstract :The present progress report on Nuclear Data Activities in India covers the work carried out during the period from July 1990 to June 1992. It contains brief description on various activities such as measurements, evaluations, compilations, processing of nuclear data, validation of nuclear data through experimental analysis and other related works being carried out in India, mainly at Bhabha Atomic Research Centre at Bombay and Indira Gandhi Centre of Atomic Research at Kalpakkam. The report gives extended abstracts of the work carried out in the above-mentioned two centres only.

70 Keywords/Descriptors : PROGRESS REPORT; RESEARCH PROGRAMS; FISSION; NEUTRON REACTIONS; ALPHA REACTIONS; FISSION PRODUCTS; FISSION YIELDS; FISSION FRAGMENTS; CROSS SECTIONS; ANGULAR DISTRIBUTION; MULTIGROUP THEORY; EXCITATION FUNCTIONS; EXPERIMENTAL DATA; INDIA; BARC; IGCAR

71	Class No. :	INIS Subject Category : G3400
99	Supplementary elements :	The previous progress report was published as BARC-1521 covering the period from January 1989 to June 1990

PREFACE

The present progress report on Nuclear Data Activities in India is the eighth report, the first of which was brought out in the year 1981. This report covers the work carried out during the period from July, 1990 to June, 1992. It contains brief description on various activities such as measurements, evaluations, compilations, processing of nuclear data, validation of nuclear data through experimental analysis and other related works being carried out in India, mainly at Bhabha Atomic Research Centre at Bombay and Indira Gandhi Centre of Atomic Research at Kalpakkam.

The work related to basic nuclear physics including nuclear structure studies and heavy ion physics being carried out at Pelletron accelerator at Bombay and Variable Energy Cyclotron at Calcutta has not been included in this report which can be found in the proceedings of the Symposium on Nuclear Physics, Vol. 35B, held at Bombay from December 21-24, 1992.

This report basically gives the extended abstracts of the work carried out and these are not to be regarded as publications or quoted without permission from authors.

S.S. Kapoor
Member, International Nuclear Data Committee

INDEX

DETERMINATION OF THE TEMPERATURE AND LEVEL DENSITY PARAMETER OF FISSION FRAGMENTS FROM MEASUREMENT OF NEUTRON ENERGY DISTRIBUTION IN $^{235}U(n_{th},f)$

M.S.Samant, R.P.Anand, R.K.Choudhury, D.M.Nadkarni and S.S.Kapoor
Nuclear Physics Division, B.A.R.C., Bombay 400 085.

Emission spectra of the prompt neutrons emitted in fission contain valuable information on the statistical properties of the fission fragments. Statistical model analysis of these emission spectra can give information on the level densities of the residual fragments after neutron emission. Details of the experimental setup and the analysis procedure to determine the neutron multiplicities and temperatures have been reported earlier/1/. In the present work the level densities of the fission fragments formed in $^{235}U(n_{th},f)$ have been inferred from the analysis of the experimentally determined fission neutron multiplicities and temperatures. Tables I and II give a summary of the experimental results on the neutron multiplicities (ν) and neutron emission spectrum temperatures (T) as a function of fragment mass (M_f) and total kinetic energy (E_K). The present results on neutron mutiplicity and temperature as a function of M_f and E_K were analysed to deduce information on the level density parameter.

The average excitation energy of fragments of specified M_f and E_K was calculated by the following relation

$$E_x(M_f,E_K) = \bar{\nu}(M_f,E_K)*[B_n(M_f) + 3/2\ T(M_f,E_K)] + E_\gamma(M_f)$$

where $B_n(M_f)$ is the neutron binding energy for the particular mass group averaged over various fragment atomic numbers, and $E_\gamma(M_f)$ is the average energy released by gamma emission. The $B_n(M_f)$ values were calculated taking into account the fragment charge distributions, and using the values of the neutron binding energies from the mass tables and the $E_\gamma(M_f)$ values were taken as half the neutron binding energy. The total excitation energies of the fragments obtained by adding the excitation energies of the complementary fragments were found to be in agreement with the estimates of excitation energies obtained from total kinetic energy measurements within about 2 MeV. The fragment excitation energy can be related to its temperature by the relation $E_x=aT^2$ where T is the fragment temperature after one neutron emission and 'a' is known as the level density parameter. The results of T^2 ($=1.2T^2_{eff}$) are plotted in Fig.1 as a function of the excitation energy per nucleon for light and heavy fragments. Two straight lines corresponding to the level density parameter a = A/7 and a = A/10 have also been drawn in these figures. Although there is a lot of scatter of the experimental points about these lines it is seen that for the light fragments, the line corresponding to a = A/7 shows the average variation of the data points, whereas for the heavy fragments the line corresponding to a = A/10 follows the average variation of the data points more closely. The above analysis indicates that the 'a' parameter for the light and the heavy fragments have different level density constants. The reason for this difference in the mass dependence of the 'a' parameter for the light and heavy fragment regions is not very clear at present and needs further investigation.

References:

/1/ M.S.Samant et al, DAE Symp.on Nucl.Phys.,Madras 33B (1990) p.131

Table I

NEUTRON MULTIPLICITY AS A FUNCTION OF FISSION FRAGMENT MASS AND TOTAL KINETIC ENERGY

TKE / MASS No.	140	145	150	155	160	165	170	175	180	185	190	195
80	.00	.00	1.16	1.24	.79	.00	.00	.00	.00	.00	.00	.00
82	.00	1.34	1.15	1.14	.93	.55	.00	.00	.00	.00	.00	.00
84	.00	1.61	1.43	1.16	1.04	.93	.58	.00	.00	.00	.00	.00
86	1.62	1.84	1.68	1.34	1.21	1.01	.81	.24	.00	.00	.00	.00
88	1.46	1.82	1.74	1.57	1.35	1.16	.84	.65	.00	.00	.00	.00
90	1.49	1.72	1.78	1.70	1.52	1.35	1.18	.89	.57	.00	.00	.00
92	1.93	2.11	2.07	1.84	1.67	1.54	1.35	1.11	.78	.00	.00	.00
94	2.20	2.12	2.16	2.00	1.81	1.64	1.46	1.19	.93	.54	.00	.00
96	2.12	2.10	2.25	2.11	1.88	1.71	1.54	1.29	1.00	.74	.00	.00
98	.00	2.55	2.36	2.24	1.99	1.83	1.63	1.33	1.07	.84	.58	.00
100	.00	2.77	2.57	2.47	2.11	1.91	1.71	1.45	1.16	.91	.66	.50
102	.00	2.63	2.63	2.46	2.25	2.08	1.83	1.52	1.33	1.07	.80	.58
104	.00	2.26	2.33	2.49	2.38	2.20	2.02	1.72	1.50	1.23	.91	.85
106	.00	1.68	3.07	2.72	2.47	2.20	2.07	1.87	1.69	1.43	1.17	1.00
108	.00	2.04	2.68	2.54	2.56	2.43	2.22	1.88	1.85	1.47	1.12	.00
110	.00	1.75	2.26	2.12	2.36	2.49	2.18	2.10	1.87	.00	.00	.00
112	.00	.00	1.94	2.01	2.29	2.22	.00	.00	.00	.00	.00	.00
114	.00	.00	1.98	1.80	1.87	.00	.00	.00	.00	.00	.00	.00
126	.00	1.94	1.55	1.09	1.05	.80	.55	.54	.38	.00	.00	.00
128	.00	1.61	1.44	1.13	.79	.83	.58	.47	.39	.36	.24	.00
130	.00	1.23	1.17	1.26	1.00	.89	.61	.53	.40	.37	.28	.22
132	.00	1.52	1.33	1.45	1.13	.96	.78	.63	.55	.46	.35	.35
134	.00	1.55	1.36	1.34	1.18	1.03	.92	.79	.69	.60	.54	.48
136	.00	1.86	1.40	1.26	1.20	1.11	.98	.84	.79	.70	.71	.64
138	.00	1.71	1.52	1.36	1.23	1.11	1.02	.93	.81	.74	.78	.00
140	1.89	1.80	1.48	1.38	1.27	1.15	1.04	.91	.78	.81	.00	.00
142	1.56	1.90	1.56	1.40	1.26	1.12	.97	.87	.79	.76	.00	.00
144	2.08	1.72	1.60	1.38	1.21	1.10	.91	.81	.75	.00	.00	.00
146	1.37	1.74	1.57	1.38	1.20	1.06	.92	.94	.82	.00	.00	.00
148	1.08	1.74	1.53	1.39	1.24	.99	.99	1.02	.00	.00	.00	.00
150	1.88	1.60	1.60	1.38	1.22	1.10	1.02	1.18	.00	.00	.00	.00
152	.00	1.59	1.38	1.26	1.18	1.13	1.25	.00	.00	.00	.00	.00
154	.00	1.48	1.38	1.48	1.10	.96	.00	.00	.00	.00	.00	.00
156	.00	.00	1.62	1.44	.79	.00	.00	.00	.00	.00	.00	.00

P

Table II

NEUTRON SPECTRUM TEMPERATURES AS A FUNCTION OF FISSION FRAGMENT MASS AND TOTAL KINETIC ENERGY

TKE / MASS No.	140	145	150	155	160	165	170	175	180	185	190	195
80			0.62	0.51								
82		0.7	0.64	0.54	0.53							
84		0.72	0.65	0.58	0.53	0.53						
86	0.71	0.59	0.54	0.63	0.56	0.49	0.33					
88	0.74	0.67	0.71	0.68	0.61	0.53	0.45					
90	0.75	0.82	0.77	0.72	0.62	0.54	0.48	0.44				
92	0.93	0.85	0.79	0.74	0.65	0.57	0.51	0.44	0.35			
94	1.00	0.91	0.78	0.78	0.70	0.60	0.53	0.46	0.40	0.35		
96		0.80	0.88	0.80	0.73	0.62	0.55	0.47	0.38	0.23		
98	1.15	0.81	0.90	0.83	0.74	0.66	0.58	0.51	0.42	0.36		
100	0.67	1.03	1.01	0.88	0.79	0.73	0.63	0.55	0.45	0.36	0.34	
102	0.48	0.52	0.98	0.94	0.88	0.77	0.67	0.59	0.52	0.43	0.36	0.34
104		0.85	0.93	0.90	0.83	0.84	0.77	0.68	0.60	0.51	0.44	0.33
106		0.78	0.75	0.88	0.85	0.90	0.83	0.76	0.66	0.58	0.52	0.40
108		0.88	0.43	0.83	0.91	0.96	0.87	0.85	0.79	0.70	0.62	0.41
110			0.50	0.77	0.95	0.96	0.92	0.93	0.85	0.77	0.65	0.55
126			0.40	0.57	0.32	0.33	0.23	0.41	0.45	0.19	0.19	
128			0.49	0.65	0.39	0.36	0.55	0.42	0.17	0.18	0.13	
130		1.05	0.51	0.75	0.68	0.80	0.52	0.48	0.39	0.34	0.39	
132		0.79	0.49	0.60	0.90	0.81	0.80	0.72	0.55	0.50	0.42	0.41
134		0.49	0.50	0.74	0.93	0.89	0.80	0.80	0.77	0.63	0.55	0.41
136		0.50	1.07	0.89	0.85	0.81	0.78	0.82	0.76	0.76	0.69	0.39
138		0.75	0.71	0.74	0.73	0.75	0.73	0.71	0.68	0.60	0.49	
140	0.82	0.59	0.76	0.71	0.70	0.71	0.68	0.64	0.55	0.56		
142	0.88	0.69	0.78	0.76	0.70	0.64	0.61	0.55	0.54	0.25		
144	0.94	0.73	0.80	0.78	0.71	0.64	0.58	0.49	0.45			
146	0.51	1.05	0.67	0.76	0.72	0.63	0.58	0.50	0.53			
148	0.49	1.04	0.83	0.75	0.72	0.63	0.60	0.48				
150	0.77	0.93	0.76	0.78	0.73	0.66	0.63	0.48				
152		1.02	0.83	0.77	0.77	0.69	0.59					
154		1.06	0.87	0.78	0.75	0.80						
156			0.54	0.88	0.72							

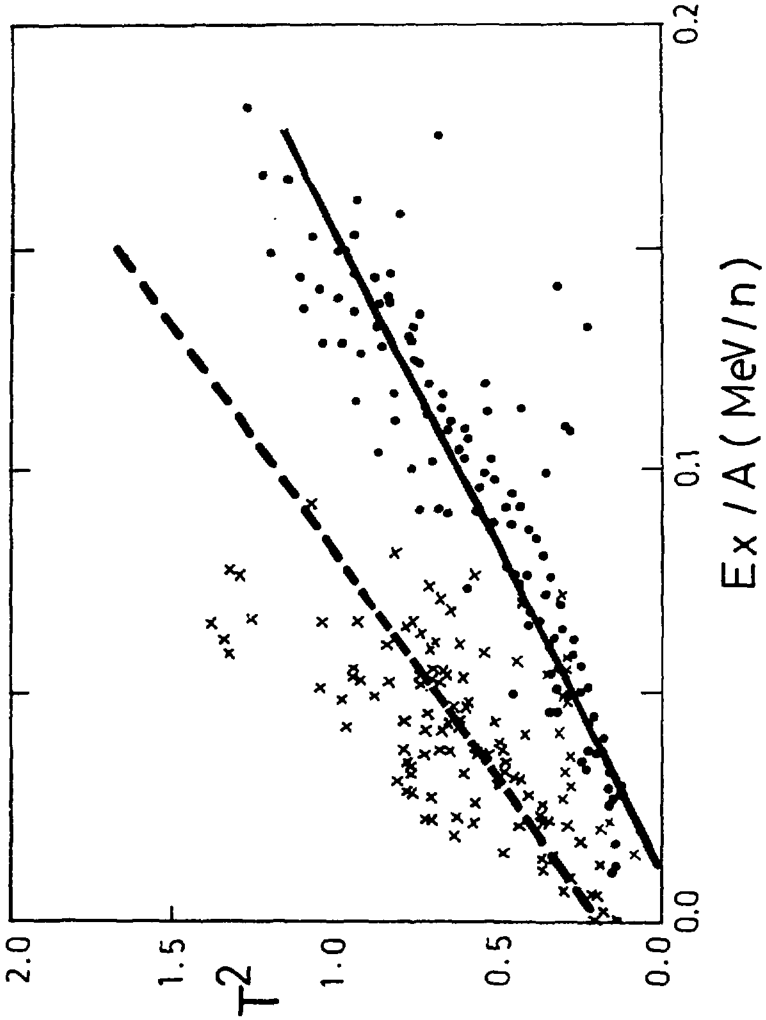

Fig.1

FISSION TIMESCALES IN $^{235}U(n_{th},f)$ FROM PRESCISSION NEUTRON MULTIPLICITY STUDIES

M.S.Samant, R.P.Anand, R.K.Choudhury, D.M.Nadkarni and S.S.Kapoor.
Nuclear Physics Division, B.A.R.C., Bombay 400 085.

Prefission neutron emission has been used as a sensitive probe for the measurement of fission timescales in fission reactions/1/. In low energy fission, the prescission neutron multiplicities can be determined from the measurement of angular distributions of neutrons with respect to the fission direction and comparing them with that expected on the basis of neutron emission from fully accelerated fission fragments. In the past there have been a number of attempts to measure the prescission neutron multiplicity (ν_{pre}) values in $^{235}U(n_{th},f)$. In the present work we have measured the ν_{pre} values in $^{235}U(n_{th},f)$ from the measurements of the neutron angular distributions as a function of fission fragment mass and total kinetic energy (E_K). Details of the experimental setup and the analysis procedure have already been reported earlier/2/. Fig.1 shows some typical measured neutron angular distributions for different kinetic energy bins for the fragment masses M_L/M_H = 96/140. The results of Monte Carlo calculations corresponding to neutron emission from fully accelerated fragments are also shown in the same figure for comparison. It is seen that the measurement and calculations agree well for low values of the fragment E_K, but with increasing fragment E_K there is a difference in the measured and the calculated neutron angular anisotropies. This difference in the measured and the calculated neutron angular anisotropy is used to estimate the ν_{pre} values. Fig.2 shows the results of the present work on the ν_{pre} values as a function of the fragment mass. It is seen that ν_{pre} does not depend on fragment mass and the average value of ν_{pre} for all fragment masses is found to be of the order of 0.18±0.05 neutrons per fission.

The average ν_{pre} value was used to estimate the saddle to scission time of the fission process in the following manner. In thermal neutron fission, the nucleus is quite cold at saddle point and acquires excitation energy during the saddle to scission transition, due to drop in the potential energy. The excitation energy of the nucleus during this time can range from 1 to 30 MeV depending upon the coupling of the collective and internal degrees of freedom/1/. For an average excitation energy of around 15MeV and the level density parameter a=A/10, the statistical neutron decay lifetime from the fissioning nucleus estimated using the statistical model code PACE II is of the order of 1.86 X 10^{-18}s. In the extreme case, assuming the excitation energy at scission point to be 30 MeV we get a neutron lifetime of 1.25 X 10^{-17}s. Thus using the measured ν_{pre} value of 0.18 and the above estimated neutron lifetimes, we get a saddle to scission time (T_f) in the range of 3 X 10^{-17}s to 2 X 10^{-20}s. These can be considered as the two limits for the timescale of the fission process. These two limits are shown in Fig.3, along with the available data in heavy ion fusion-fission reactions for various fissioning systems. It is seen that the present results agree with the systematic trend obtained for all the systems.

References:

/1/S.S.Kapoor,Proc.INDC Meeting on the Physics of Neutron Emission in Fission,Mito City, Japan, IAEA, June 1989, INDC-(NDS)-220,p 207

/2/M.S.Samant et al,DAE Symp.on Nucl.Phys.,Bombay34B (1991)p.231

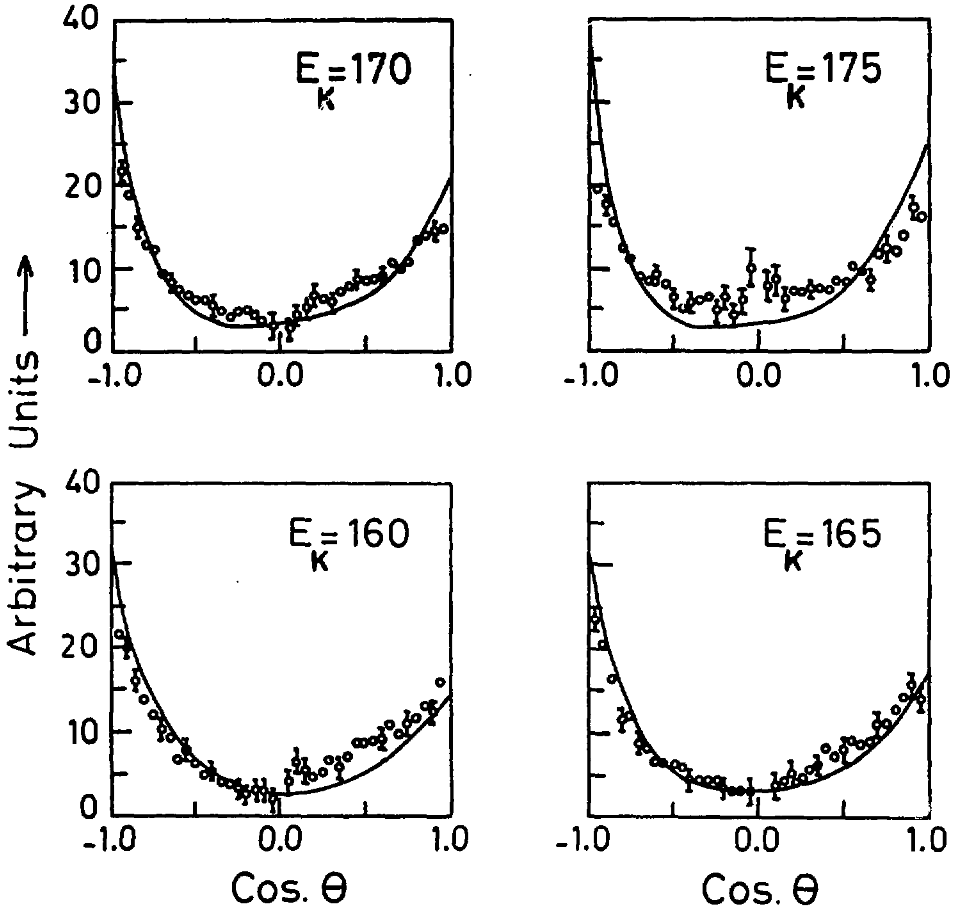

Arbitrary Units
$E_K = 170$
$E_K = 175$
$E_K = 160$
$E_K = 165$
40
30
20
10
0
-1.0
0.0
1.0
Cos. Θ

Fig. 1

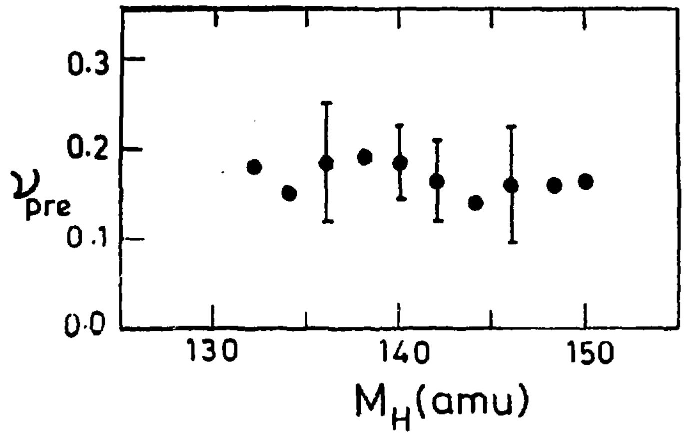

Fig. 2

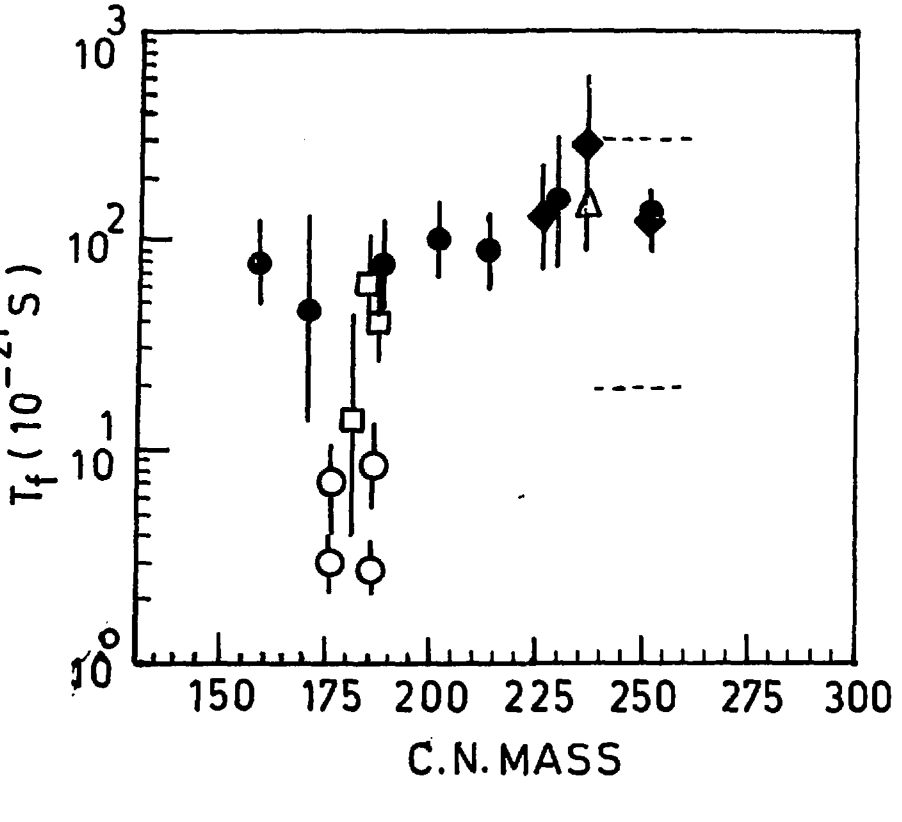

Fig. 3

Excitation function and fragment angular distributions in the fission of Au-197 induced by He-ions in the energy range of 30 - 70 MeV

P.C.Kalsi, A.K.Pandey, R.C.Sharma and R.H.Iyer
Radiochemistry Division , BARC
Trombay, Bombay - 400 085, INDIA

The fission cross sections and fragment angular distributions in the fission of Au-197 (Z=79) excited with He-ions in the energy range 30-70 MeV have been measured using the sensitive fission track technique. The measured fission cross sections vary from 11 microbarns at 30 MeV to 16.8 millibarns at 70 MeV. The data were analysed using a statistical model expression to get the fission barrier, E_f of Tl-201 (compound nucleus formed by the interaction of Au-197 and He-ion) and the level density parameters, a_n and a_f for neutrons emission and fission respectively.

The experimental values are : E_f = 19.3 ± 2.5 MeV : a_f = 16.75 MeV^{-1} ; a_n = 14.57 MeV^{-1}. These values agree very well with the best data available in the literature. The angular distribution data is being analysed to understand the variation of anisotropy ratios with the excitation energy of the compound nucleus and to get information on the spin distribution and shape of the nucleus at the saddle point.

Table - 1

$^{4}He + ^{197}Au\ (\alpha,f)$

E_L (MeV)	E_x (MeV)	$\sigma_f (cm^2)$		$\sigma_R (cm^2)$	Experimental Anisotropy $W_{180°}/W_{90°}$
		Integral method	Absolute method	Optical Model	
70	67.4	16.79 X 10^{-27}	20.11 X 10^{-27}	22.59 X 10^{-25}	1.89
65	62.5	9.46 X 10^{-27}	10.96 X 10^{-27}	22.06 X 10^{-25}	2.21
60	57.6	7.74 X 10^{-27}	8.99 X 10^{-27}	21.42 X 10^{-25}	1.71
55	52.7	3.20 X 10^{-27}	4.81 X 10^{-27}	20.62 X 10^{-25}	1.80
50	47.8	2.19 X 10^{-27}	2.63 X 10^{-27}	19.62 X 10^{-25}	1.63
45	42.9	6.06 X 10^{-28}	7.17 X 10^{-28}	18.34 X 10^{-25}	2.13
40	38.0	19.50 X 10^{-29}	20.92 X 10^{-29}	16.67 X 10^{-25}	1.90
35	33.1	29.30 X 10^{-30}	28.3 X 10^{-30}	14.42 X 10^{-25}	1.76
30	28.2	11.55 X 10^{-30}	12.45 X 10^{-30}	11.30 X 10^{-25}	2.50

Published in
1- DAE Symposium on Radiochem. & Radiation Chem., Nagpur University, Nagpur, Feb. 5-8 (1990).
2- 7 th National Conference on Particle Tracks in Solids, Defense Laboratory, Jodhpur, Oct. 9-11 (1991).

Fission excitation function of ^{181}Re compound nucleus formed by $^{12}C + ^{169}Tm$ and $^{16}O + ^{165}Ho$ reactions.

A.K.Pandey, P.C.Kalsi, R.C.Sharma and R.H.Iyer
Radiochemistry Division , BARC
Trombay, Bombay - 400 085, INDIA

With a view to understanding the effect of angular momentum on fission barrier and fragment anisotropy we have measured the fission cross sections and fragment angular distributions of the $_{75}^{181}Re$ compound nucleus produced by $_6^{12}C+_{69}^{169}Tm$ and $_8^{16}O+_{67}^{165}Ho$ reactions at several bombarding energies above the fusion barriers. In particular , we have chosen lower energies where no experimental data are available and where the average angular momentum of the $^{16}O+^{165}Ho$ systems is lower than that of the $^{12}C+^{169}Tm$ system the cross over occurring at an excitation energy of about 57.6 MeV and $\langle l \rangle_{av}$ about 27.5 $\hbar$.
Statistical model fits to the experimental excitation functions were performed by using angular-momentum-dependent fission barriers $E_f(J)$ from Rotating Liquid Drop Model (RLDM) and from the rotating finite range model RFRM of Sierk at different $\langle l \rangle_{av}$ values. Evaporation residue cross sections $_{ER}$ rather than total reaction cross sections $_R$ (optical model) were used to get Γ_f/Γ_n values. It is seen that best fits to the experimental data are provided by using the $E_f(J)$ from RFRM. The predicted cross sections are much smaller with $E_f(J)$ from RLDM.
Our data are consistent with RFRM $E_f(J=0)$ value of 19.2 MeV for ^{181}Re. The RLDM $E_f(J=0)$ value of 22 MeV is high and is inconsistent with the experimental data. Another noteworthy observation is the excellent correspondence between the variation of $\langle l \rangle_{av}$ of $^{12}C+^{169}Tm$ and $^{16}O+^{165}Ho$ and the Γ_f/Γ_n values with excitation energy. The cross-over point (E=57.6 MeV and $\langle l \rangle_{av}$ 27.5 $\hbar$) represents a true compound nucleus with out any entrance channel effects. Further measurements of σ_f and $d\sigma/d\Omega$ on the ^{181}Re and other systems at excitation energies close to the cross-over region are in progress.

TABLE

SYSTEM	E_L MeV	E_x MeV	σ_f mb
$^{16}O+^{165}Ho$	81	50.7	.020
	83	52.5	.078
	85	54.3	.106
	100	68.0	6.34
$^{12}C+^{169}Tm$	70.2	50.7	.104
	72.1	52.5	.171
	74.0	54.3	.255
	79.0	58.9	1.13
	82.0	61.7	1.84

Published in
1- DAE Symp. on Nuclear Physics, Proc. of the vol. 34B, page no. 13., Bombay (1991).

^{16}O-Ion-Induced Fission Of ^{197}Au

A.K.Pandey, P.C.Kalsi, R.C.Sharma and R.H.Iyer
Radiochemistry Division , BARC
Trombay, Bombay - 400 085, INDIA

Analysis of the fission excitation function of ^{213}Fr compound nucleus formed by the $^{16}O+^{197}Au$ using angular-momentum-dependent fission barriers has confirmed the validity of Rotating Finite Range Model (RFRM) in reproducing the experimental excitation functions with the estimated fission barrier E_f (J=0) value of 7.62 MeV for ^{213}Fr. The experimental anisotropies at different energies of ^{16}O were compared with those calculated by Standard Statistical Saddle Point Model.The experimental anisotropy data are consistent with those obtained by SSPM.The measurements were done by using the Lexan plastic detector.

Table

E_L MeV	σ_f mb	$W_{180°}/W_{90°}$ (Exp.)	$W_{180°}/W_{90°}$ (Cal.)
75	.112	1.24±.02	1.224
81	18.1	1.76±.14	1.348
96	420	2.66±.21	2.464
108	919	2.90±.15	3.068

Published in
1- DAE Symp. on Nuclear Physics, Univ. of Madras, Madras (1990), Paper No. 024.

2- DAE symposium on Nuclear and Radiochemistry, Andhra University, Visakhapatnam , Dec 21-24 (1992)

Excitation Functions Of ^{4}He-Ion-Induced Fission Of ^{159}Tb And $^{nat.}Yb$

A.K.Pandey, P.C.Kalsi, R.C.Sharma and R.H.Iyer
Radiochemistry Division , BARC
Trombay, Bombay - 400 085, INDIA

Experimental work on the helium ion induced fission excitation functions of Tb^{159} (Z=65) and $Yb^{173.1}$ (Z=70) have been completed. The fission cross sections σ_f and the total reaction cross section σ_R obtained from these experiments are summarized below

TABLE-1 Experimental fission cross sections

He^4 ion energy (MeV)	Target	Excitation energy (MeV)	σ_f (cm^2)	σ_R (cm^2)	$\Gamma_f/\Gamma_R \approx \sigma_f/\sigma_R$
47.5	Tb^{159}	45.6	$(4.16\pm0.91)10^{-33}$	1.910×10^{-24}	2.178×10^{-9}
50.0		48.0	$(1.54\pm0.28)10^{-32}$	1.954×10^{-24}	7.866×10^{-9}
55.0		52.9	$(4.19\pm0.48)10^{-32}$	2.026×10^{-24}	2.069×10^{-8}
60.0		57.8	$(1.53\pm0.11)10^{-31}$	2.083×10^{-24}	7.331×10^{-8}
40.0	$Yb^{173.1}$	36.9	$(1.55\pm0.22)10^{-32}$	1.722×10^{-24}	9.001×10^{-9}
42.5		39.3	$(4.52\pm0.56)10^{-32}$	1.796×10^{-24}	2.517×10^{-8}
45.3		42.0	$(8.30\pm0.91)10^{-32}$	1.860×10^{-24}	4.462×10^{-8}
50.0		46.6	$(1.20\pm0.07)10^{-30}$	1.965×10^{-24}	6.107×10^{-7}
55.0		51.5	$(2.58\pm0.08)10^{-30}$	2.047×10^{-24}	1.236×10^{-6}
60.0		56.4	$(8.90\pm0.31)10^{-30}$	2.112×10^{-24}	4.214×10^{-6}
65.0		61.3	$(1.45\pm0.03)10^{-29}$	2.164×10^{-24}	6.701×10^{-6}

The data were analyzed using the statistical model .The experimental fission barriers of ^{163}Ho and $^{177.1}Hf$ obtained by analysis of excitation functions were compared with fission barriers calculated by theoretical models such as the simple liquid drop model (LDM) , rotating liquid drop model (RLDM) , shell-corrected liquid drop model and rotating finite range models (RFRM) of Sierk and Mustafa et.al. These are summarized in the table given below . There are good agreement between the measured experimental fission barriers and those predicted by a semi-empirical mass formulation based on the charged liquid drop. This indicates that ground state deformation has very little effect on the lowering of the fission barriers.

Table:- Experimental & theoretical fission barriers (MeV)

C.N.	EXP.E_f	L.D.M.	R.L.D.M.	Sh.-Corr.L.D.	Sierk	Mustafa
$_{67}Ho^{163}$	31.5±3.5	36.98	33.6	34.3	28.4	30.5
$_{72}Hf^{177.1}$	26.7±3.0	30.60	27.3	28.6	23.3	25.3

Our fission barrier data on the compound nuclei ^{163}Ho, $^{171.3}Yb$, ^{169}Tm and $^{177.1}Hf$ along with similar data available in the literature have been used to bring out some interesting predictions concerning the trends and systematics of symmetric and asymmetric fission barriers in lighter and heavier nuclei.

One of the most interesting results arising out of the present analysis is the striking linear relationship between $\log_{10} \Gamma_f/\Gamma_n$ normalised to a constant excitation energy of 40 MeV and Z^2/A for the compound nuclei from ^{163}Ho to ^{213}At where symmetric fission is predominant which can be represented by the equation

$$\mathrm{Log}_{10}\Gamma_f/\Gamma_n = 1.262 Z^2/A - 44.77 \qquad \ldots\ldots (1)$$

However, in the actinide regions ranging from ^{232}Th-^{254}Fm (all of which are predominantly asymmetric fission nuclei), only a relatively weak dependence of $\log_{10} \Gamma_f/\Gamma_n$ on Z^2/A was observed which can be represented by the equation

$$\mathrm{Log}_{10} \Gamma_f/\Gamma_n = 0.366\ Z^2/A - 13.455 \qquad \ldots\ldots (2)$$

A theoretically more meaningful analysis may be the correlation of Γ_f/Γ_n with $E_f'-B_n'$ where E_f' and B_n' are effective fission barrier and neutron binding energy respectively. Based on minimum sum of squares of deviation, 50% shell correction with pairing energy term was found to best represent the data and can be represented by the following equation:

$$\mathrm{Log}_{10}\Gamma_f/\Gamma_n = 1.593 - 0.452\ (E_f'-B_n') \qquad \ldots\ldots (3)$$

The results suggest that shell effects tend to persist even at higher excitation energy .
On combining equation (1) and (3) the following equation is obtained.

$$E_f' - B_n' = 102.57 - 2.79\ Z^2/A \qquad \ldots\ldots. (4)$$

If one neglects, or averages out shell effects, and assumes B_n' is approximately constant, then

$$E_f = K_1 - K_2\ (Z^2/A) \qquad \ldots.. (5)$$

where K_1 and K_2 are constants. This is the same form given by Cohen and Swiatecki for obtaining the barrier of a charged liquid drop. Since the equation (4) represents symmetric fission, the E_f' in the above equation can be assumed to be $E_f'_{(symmetric)}$. The symmetric fission barriers obtained from the above equation were compared with the experimental symmetric fission barriers available in the literature .(Table-1) **It is obvious from these results that the symmetric fission barrier obtained from equation 4 are reasonably close to experimentally observed fission barrier.** From the limited available data on asymmetric fission barriers , it is apparent that asymmetric fission barrier $(E_f'_{(asy)} - B_n')$ is linearly dependent on Z^2/A. Based on the available data, the asymmetric fission barrier can be represented by the equation.

$$E_f'_{(asym)} - B_n' = 235.11 - 6.65\ Z^2/A \qquad ....(6)$$

From table , it appears that near A=200, the asymmetric fission barrier may become so much higher than symmetric fission barrier that asymmetric fission may not be experimentally observable below A ≈ 200 and hence it disappears around A ≈ 200.

Table Symmetric and asymmetric fission barriers

Nuclide	Symm. fission barrier [From eq.4] MeV	Exp. symm. fission barrier MeV	Asymm. fission barrier [From eq.6] MeV	Exp. Asymm. fission barrier MeV	Average Exp. fission barrier* MeV
^{163}Ho	31.66	--	57.90	--	31.5
^{169}Tm	30.01	--	53.90	--	29.6
$^{171.3}Yb$	29.00	--	51.14	--	27.8
^{173}Lu	27.62	--	47.68	--	28.7
$^{177.1}Hf$	27.01	--	46.57	--	26.7
^{201}Tl	21.47	--	28.02	--	22.5
^{210}Po	20.67	21.2	23.51	24.4	20.4
^{213}At	15.43	17.3	17.04	19.8	16.8
^{227}Ra	11.89	9.3	12.06	7.95	--
^{226}Ac	8.65	8.8	5.98	7.80	--
^{227}Ac	9.59	8.5	7.45	7.40	--
		8.5		7.30	--
^{228}Ac	9.02	8.8	7.47	7.0	--
		9.2		7.2	
^{232}Th	9.93	--	7.71	--	5.95
^{233}Th	9.50	--	7.87	--	6.44
^{232}Pa	6.87	--	1.65	--	6.18
^{238}U	8.26	--	3.54	--	5.80

*** Obtained by analysis of excitation functions.**

Published in

1- Physical Review C, Vol. 44, No. 6, 2644-2652 (1991).
2- DAE Symp. on Nuclear Physics, Proc. of the vol. 34B, page no. 213., Bombay (1991).
3- DAE symposium on nuclear physics , BARC , Bombay, Dec. 21-24, 1992
4- Communicated to Physical Review C.

Alpha particle induced reactions on ^{27}Al at 55.2 and 58.2 MeV

S.S.Rattan, A.Ramaswami, R.J.Singh and Satya Prakash

Radiochemistry Division, Bhabha Atomic Research Centre,
Bombay-400 085, India

The alpha particle induced reactions on ^{27}Al have been studied using gamma ray spectrometry. The cross sections for the formation of ^{7}Be, ^{22}Na, ^{24}Na, ^{27}Mg, ^{28}Mg, ^{28}Al and ^{29}Al in the alpha particle induced reaction on ^{27}Al with alpha particles of energy 55.2 MeV and 58.2 MeV have been determined. The results are discussed in terms of increasing projectile energy and multi nucleon as well as cluster emission from the excited nucleus.

Table 1. Experimental cross section in mb for the production of ^{7}Be, ^{22}Na, ^{24}Na, ^{27}Mg, ^{28}Mg, ^{28}Al and ^{29}Al by irradiation on ^{27}Al with alpha particles.

Reaction products	Cross section in mb at alpha particle energies				
	55.6 MeV [Ref.1]	58.8 MeV [Ref.1]	58 MeV [Ref.2]	55.2 MeV Present	58.2 MeV Present
^{7}Be	0.96	1.32	1.0	1.025	1.136 ± 0.054
^{22}Na	48.93	46.2	49.	49.77 ± 0.82	43.98 ± 1.63
^{24}Na	15.11	22.56	18.	12.37 ± 0.76	18.54 ± 0.54
^{27}Mg	--	--	5.4	2.34 ± 0.07	3.01 ± 0.12
^{28}Mg	0.46	0.60	0.43	0.435 ± 0.039	0.410 ± 0.032
^{28}Al	--	--	--	74.66 ± 8.73	71.94 ± 11.35
^{29}Al	--	--	6.6	5.81 ± 0.54	5.37 ± 0.31

Published in Radiochimica Acta 51, 55-57 (1990)

For references, see above publication.

Alpha Particle Induced Fission of ^{209}Bi at 55.7 and 58.6 MeV

S.S.Rattan, A.Ramaswami, R.J.Singh and Satya Prakash,
Radiochemistry Division, Bhabha Atomic Research Centre,
Bombay-400085, India

The alpha particle induced fission studies of ^{209}Bi have been carried out at alpha particle energies of 55.7 MeV and 58.6 MeV using gamma ray spectrometry. The cross sections for the production of fission products have been determined. The mass distributions have been found to be broad with a peak near mass 104. The charge distribution in the alpha particle induced fission of ^{209}Bi has been studied at alpha particle energies of 55.7 MeV and 58.6 MeV. The fractional cumulative yields of ^{97}Zr, ^{99}Mo, ^{101}Mo, ^{112}Pd and ^{117m}Cd have been determined using gamma ray spectrometry. The width of charge distribution has been found to be broad.

Table 1. Experimental cross sections in μb for the formation of fission products in the alpha particle induced fission of ^{209}Bi.

Fission Product	44.9 MeV (Ref. [8,9])	49.1 MeV (Ref. [8,9])	55.7 MeV This work	58.6 MeV This work
^{85m}Kr		173 ± 48		678 ± 40
^{91}Sr	395 ± 38		738 ± 297	1026
^{92}Sr		450 ± 158	1218	1399 ± 232
^{95}Zr		793 ± 72		
^{97}Zr		715 ± 150	1459 ± 563	1650 ± 330
^{99}Mo	497 ± 35	918 ± 95	1564 ± 518	2121 ± 587
^{101}Mo			3790 ± 242	3640 ± 522
^{103}Ru	653 ± 95	1109 ± 170	1366	2235 ± 465
^{104}Tc		804 ± 80	1850 ± 1073	1900 ± 481
^{105}Ru		990 ± 67	2489 ± 1892	2883 ± 265
^{107}Rh			2133 ± 1195	2125 ± 553
^{111}Ag			1122	1614 ± 537
^{112}Pd	483 ± 68	657 ± 66	1792 ± 769	2035 ± 485
^{115}Cd		382 ± 77	1023 ± 401	1185 ± 224
^{117m}Cd			920 ± 500	844 ± 349

Table 2. Experimental fractional cumulative yields and calculated Zp values in the alpha particle induced fission of ^{209}Bi at alpha particle energy of 55.7 MeV and 58.6 MeV.

Parent Nuclide	Gamma ray energy of daughter in keV	FCY and Zp at alpha particle energy of ---- 55.7 MeV ---- FCY	Zp	--- 58.6 MeV ---- FCY	Zp
^{97}Zr	657.9	0.667±0.039	39.86	0.589 ±0.111	39.93
^{99}Mo	140.5	0.878±0.011	40.67	0.763 ±0.174	40.75
^{101}Mo	306.8	0.655±0.134	41.49	0.688 ±0.114	41.56
^{112}Pd	617.4	--	45.96	0.599 ±0.015	46.03
^{117m}Cd #	158.6, 553.0	0.798±0.169	47.83	0.791 ±0.130	47.91

\# The FCY value of ^{117m}Cd is partial because here only m state of ^{117}Cd is involved.

Table 3. Total fission cross section in mb in the alpha particle induced fission of ^{209}Bi at alpha particle energy of 55.7 MeV and 58.6 MeV.

Alpha particle energy in MeV	Total fission cross section in mb (Ref. [7])	Present	Average FCY used
55.7	64	66	0.733
58.6	88	88	0.660

Published in Radiochimica Acta 55, 169-172 (1991).

For references, see above publication.

Alpha Particle Induced Reactions of ^{209}Bi at 55.7 and 58.6 MeV

S.S.Rattan, N. Chakravarty, Ramaswami and R.J.Singh,
Radiochemistry Division, Bhabha Atomic Research Centre,
Bombay-400085, India

The alpha particle induced reaction studies of ^{209}Bi have been carried out at alpha particle energies of 55.7 MeV and 58.6 MeV using gamma ray spectrometry. The cross sections for the production of reaction products ^{207}At, ^{208}At, ^{209}At and ^{210}At have been determined. The variation of experimental production cross section for the reaction products in $^{209}Bi(\alpha,xn)^{213-x}At$ as a function of neutron number of the reaction products at different available energies showed the presence of possible shell effects at neutron number 126.

Table 1. Experimental cross section in mb for the production of ^{207}At, ^{208}At, ^{209}At and ^{210}At by irradiation of ^{209}Bi with alpha particles

Energy in MeV	^{207}At	^{208}At	^{209}At	^{210}At
55.7	37.2	904 $\pm$ 65	1135 $\pm$ 31	231 $\pm$ 7
58.6	55.1 $\pm$ 10.4	893 $\pm$ 85	493 $\pm$ 37	123 $\pm$ 7

Published in Radiochimica Acta 57, 7-9 (1992).

Table 2. Calculated lab energy and the corresponding experimental production cross section for reaction products in $^{209}Bi(\alpha,xn)^{213-x}At$ as a function of neutron number of the reaction products at different available energies

Reaction product	^{207}At	^{208}At	^{209}At	^{210}At	^{211}At	^{212}At
Reaction	$(\alpha,6n)$	$(\alpha,5n)$	$(\alpha,4n)$	$(\alpha,3n)$	$(\alpha,2n)$	(α,n)
Neutron number	122	123	124	125	126	127
Q-value	-50.99	-43.65	-35.24	-28.08	-20.33	-15.29
Available energy (E_{av})	Calculated lab energy in MeV and the corresponding experimental production cross section in mb for reaction products in $^{209}Bi(\alpha,xn)^{213-x}At$					
1.0	52.99	45.51	36.93	29.63 (8)	21.73 (33)	16.54 (0.2)
2.0	54.01	46.53	37.95	30.65 (52)	22.75 (115)	17.56 (1.0)
3.0	55.03	47.54 (14)	38.97 -	31.67 (160)	23.77 (240)	18.58 (5.8)
4.0	56.05 (39)	48.56 (39)	39.99 -	32.69 (325)	24.79 (390)	19.60 (25)
5.0	57.06 (45)	49.58 (80)	41.01 (151)	33.71 (560)	25.81 (520)	20.62 (76)
6.0	58.08 (51)	50.60 (120)	42.03 (230)	34.73 (780)	26.83 (640)	21.63 (132)
7.0	59.10 -	51.62 (180)	43.05 (345)	35.75 (920)	27.85 (740)	22.65 (140)
8.0	60.12 -	52.64 (270)	44.07 (570)	36.77 (1020)	28.87 (810)	23.67 (109)
9.0	61.14 -	53.66 (405)	45.09 (990)	37.78 (1140)	29.89 (870)	24.69 -
10.0	62.16 -	54.68 (620)	46.10 (910)	38.80 (1180)	30.91 (900)	25.71

Note:- The number in the brackets are the corresponding experimental production cross section for reaction products in $^{209}Bi(\alpha,xn)^{213-x}At$.

ANGULAR DISTRIBUTION IN ALPHA-INDUCED FISSION OF 232Th and 238U

T.Datta, S.P.Dange, H.Naik and S.B.Manohar

Radiochemistry Division, Bhabha Atomic Research Centre,
Trombay, Bombay-400 085, INDIA.

Angular distribution of fission products have been measured as a function of mass asymmetry in the fissioning systems $^{232}Th(\alpha_{39.1MeV},f)$, $^{238}U(\alpha_{29.0MeV},f)$ and $^{238}U(\alpha_{39.1MeV},f)$ using recoil-catcher technique and off-line gamma spectrometry. Present data have been analysed alongwith similar data reported earlier by us in $^{232}Th(\alpha_{29MeV},f)$ and $^{233}U(\alpha_{29MeV},f)$ and literature data on mass-averaged products in the same fissioning systems in the alpha energy region 16 to 40 MeV.

Angular anisotropies of the average symmetric and asymmetric products in all these fissioning systems have been evaluated based on the transition state model assuming two fission modes with characteristic shapes and barrier heights and considering multichance fission at various alpha energies. Agreement between the calculated and experimental anisotropies indicate that the angular distributions for the symmetric and asymmetric modes are decided at and well past the corresponding second saddles in the deformation energy surface. Effects of multichance fission is also seen to play a significant role depending on the properties of the nuclides concerned.

Table-1 :Anisotropy values for Symmetric and Asymmetric modes in $^{232}Th(\alpha,f)$ and $^{238}U(\alpha,f)$.

Fissioning System:	$^{232}Th + \alpha$		$^{238}U + \alpha$	
E_{α} (MeV)	29.0	39.0	29.0	39.0
E^{*} (MeV)	23.5	33.3	23.4	33.3
$\langle J \rangle$ $\hbar$	9.1	13.7	9.8	13.7
LAB. System:				
W(0)/W(90)	1.38	1.62	1.37	1.54
:Symmetry	±0.13	±0.10	±0.10	±0.06
W(0)/W(90)	1.68	1.96	1.66	1.78
:Asymmetry	±0.09	±0.11	±0.12	±0.09
C>M> System:				
W(0)/W(90)	1.26	1.48	1.25	1.41
:Symmetry	±0.11	±0.09	±0.09	±0.06
W(0)/W(90)	1.55	1.80	1.52	1.63
:Asymmetry	±0.09	±0.10	±0.11	±0.08

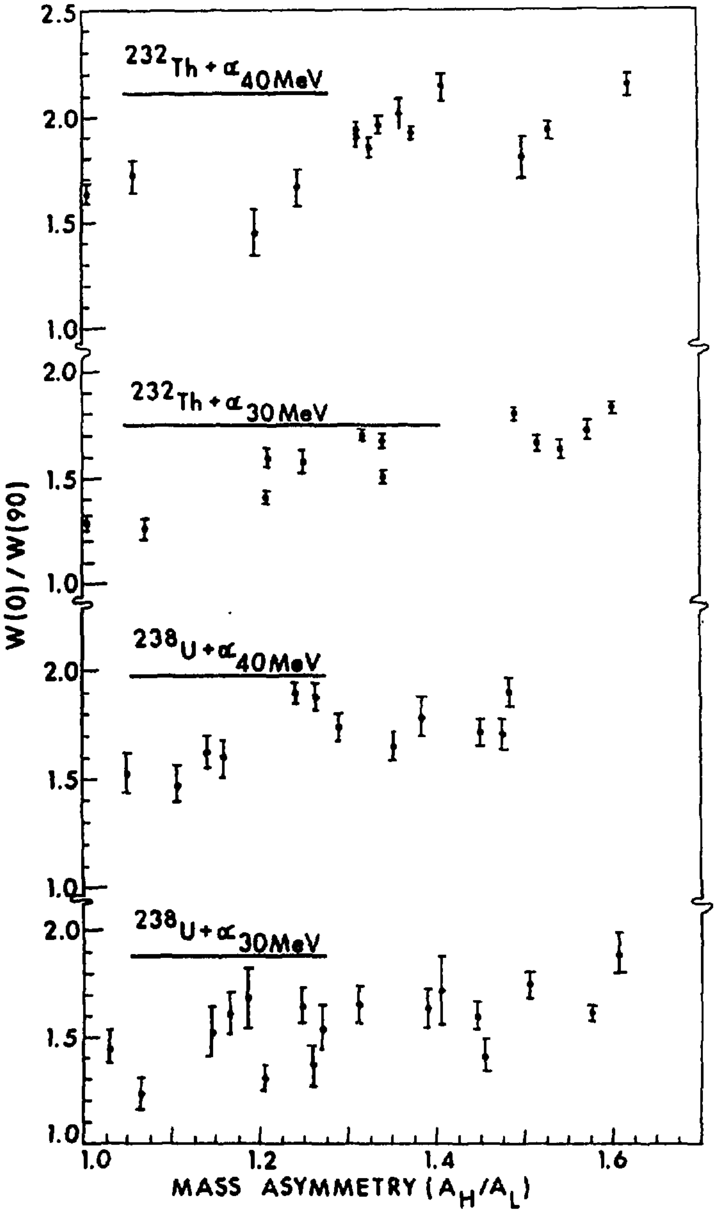

FIG.-1. EXPERIMENTAL ANGULAR ANISOTROPY AS A FUNCTION OF FISSION PRODUCT MASS ASYMMETRY.

EMISSION ANGLE DEPENDENCE OF FISSION FRAGMENT SPIN.

T.Datta, S.P.Dange, H.Naik and Satya Prakash
Radiochemistry Division, Bhabha Atomic Research centre,
Trombay,Bombay-400085, INDIA.

Average spin of fission fragment at specific mass-asymmetry has been obtained as a function of emission angles in $^{238}U(\alpha_{39.1MeV},f)$system from radiochemically determined independent isomeric yield ratios of ^{132}I. Fragment average spin is seen to decrease from 11.2 to 6.5 $\hbar$ with change in emission angle from 90° to 20°, due to the angle dependent tilting component over-and-above the statistical wriggling, bending and twisting components as per the collective mode model. Effects of entrance channel parameters and multichance fission are also discussed.

Ref: Phys. Rev. C-46, 1445 (1992). : Table-2.

A. Fragment Angular Momentum Studies in Fission:
Technique: Radiochemically determined Independent Isomeric Yield Ratio + Statistical model of Spin Distribution.

Table-1. Fissioning System $^{238}U(\alpha,f)$: as a function of energy.
Fission Product Isomer: $^{132m,g}I$.

Eα(MeV)	Ex(MeV)	Yield Ratio	Jrms(ħ)
25.2	14.8	0.59±0.08	10.1±1.4
27.0	16.0	0.68±0.06	12.2±1.3
33.1	20.6	0.76±0.05	14.3±1.6
39.1	25.2	0.76±0.05	14.4±1.5
44.2	29.7	0.78±0.04	15.4±1.5

* Ref: H.Naik, T.Datta, S.P.Dange, R.Guin, P.K.Pujari, S.M.Sahakundu and SatyaPrakash; Z.Phys.A-342,95(1992).

Table-2. Fissioning System $^{238}U(\alpha,f)$: as a function of angles.
Fission Product Isomer: $^{132m,g}I$.
Eα=39 MeV. Ex=33.2 MeV. <I>= 14.6 ħ

θ(deg)	Δθ(deg)	Yield Ratio	<J> ħ expt.	<J> ħ Theor.[CMM]
84.5	10.9	0.81±0.01	11.2±0.4	11.5
64.2	8.5	0.80±0.02	10.8±0.4	10.8
48.9	6.3	0.70±0.04	8.3±0.8	9.9
38.5	4.3	0.62±0.03	7.2±0.4	9.2
31.3	3.4	0.55±0.03	6.5±0.3	8.8
25.7	8.6	0.56±0.02	6.5±0.3	8.5

*Ref: T.Datta, S.P.Dange, H.Naik and SatyaPrakash; Phys.Rev. C-46,1445(1992).

Table-3. Fissioning Systems: $^{232}Th(\alpha,f)$ AND $^{232}Th(p,f)$.
: As a function of Kinetic Energy and Emission Angles.
Fission Product Isomer: $^{132m,g}I$.

System	$^{232}Th(p,f)$		$^{232}Th(\alpha,f)$	
Ex(MeV)	23.2		33.2	
<I> ħ	4.8		14.6	
Al- Catcher Thickness(micron)	7.6	25.0	7.6	25.0
<θ>cut-off	43.0°		45.0°	
<J> ħ	12.1 ±1.2	8.9 ±0.5	15.6 ±1.2	9.5 ±0.5

*Ref: T.Datta, S.P.Dange, H.Naik, S.B.Manohar; DAE Symp. on Nuclear Physics,BARC(1992).

Table-4. Fissioning System $^{245}Cm(n,f)$

Fission Product	Yield Ratio	Jrms($\hbar$)	TKE(MeV) deduced	TKE(MeV) expt.
131-Te	0.70±0.06	6.1±0.7	194.5	194.9
133-Te	0.56±0.05	4.6±0.4	193.0	198.4
135-Xe	0.68±0.06	5.8±0.6	190.5	190.6

* Ref: H.Naik, S.P.Dange, T.Datta., DAE Symp. on Nuclear and Radiochemistry, Waltair(1992).

B. Charge Distribution Studies in Low Energy Fission.

Table-1. Fractional Cumulative and Independent yields(132-I) in the mass chains 128,131,132 and 134 in netron induced fission of Actinides.

Actinide.	128-Sn	131-Sb	132-Te	134-Te	132-I
233-U	0.78±0.10	0.56±0.04	0.96±0.04	0.62±0.03	0.18±0.01
235-U	0.94±0.04	0.80±0.02	0.99±0.01	0.89±0.02	0.02±0.01
239-Pu	0.85±0.10	0.65±0.02	0.95±0.01	0.67±0.01	0.16±0.01
241-Pu	0.93±0.04	0.78±0.03	0.99±0.01	0.84±0.01	0.03±0.01
245-Cm	0.75±0.05	0.65±0.03	0.94±0.02	0.56±0.02	0.23±0.04

*Ref; H.Naik, S.P.Dange, T.Datta; Radiochim. Acta(1993).(in press).

MASS RESOLVED ANGULAR DISTRIBUTION IN HELIUM ION INDUCED FISSION OF ^{233}U

A.Goswami, S.B.Manohar, S.K.Das, A.V.R.Reddy.
B.S.Tomar and Satya Prakash
Radiochemistry Division, Bhabha Atomic Research Centre
Bombay 400085, INDIA

Angular distribution of eight fission profucts were determined by recoil catcher technique and direct gamma spectrometry in the 28.5 MeV alpha induced fission of ^{233}U. The data were fitted with standard angular distribution function to obtain the angular anisotropies. Table-1 gives the angular anisotropies for the fission products. The angular anisotropies of asymmetric fission products were found to be higher than those of symmetric products (figure-1) indicating a correlation between the fragment angular distribution and the mass distribution.

References:

1. A.Goswami, S.B.Manohar, S.K.Das, A.V.R.Reddy, B.S.Tomar, and Satya Prakash Z.Phys. A 342, 299 (1992)

Table 1.
Angular anisotropies of fission fragments in $^{233}U(\alpha,f)$ at E_{α}=28.5MeV

Nuclides	Angular anisotropy W(0)/W(90)
^{97}Zr	1.35 ± 0.08
^{99}Mo	1.34 ± 0.08
^{105}Rh	1.36 ± 0.08
^{112}Pd	1.22 ± 0.06
^{115g}Cd	1.23 ± 0.09
^{131}I	1.45 ± 0.09
^{132}Te	1.42 ± 0.09
^{143}Ce	1.36 ± 0.08

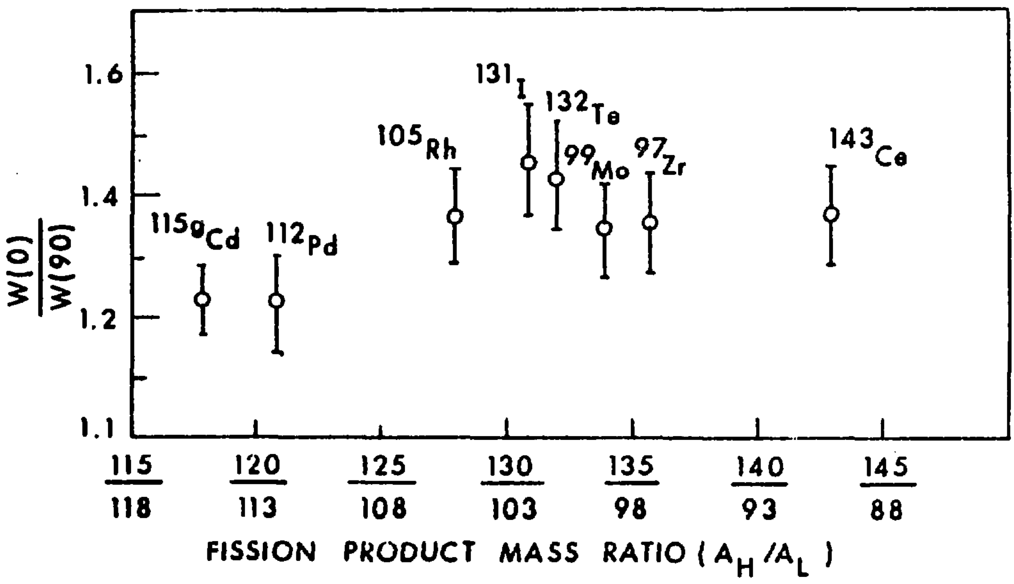

FIG. - 2. DEPENDENCE OF ANGULAR ANISOTROPY ON MASS RATIO.

Mass distribution in ^{12}C induced fission of ^{232}Th

S.B. Manohar. A. Goswami, A.V.R. Reddy, B.S. Tomar,
P.P. Burte and Satya Prakash
Radiochemistry Division, Bhabha Atomic Research Centre
Bombay 400 085, India.

Cumulative/ independent cross-sections of 25 fission products were determined in the 79 MeV ^{12}C induced fission of ^{232}Th using recoil catcher technique and spectrometry. These were used to deduce to mass yields using the charge distribution parameters which were estimated from the independent cross-sections of the shielded nuclides ^{122}Sb, ^{124}Sb and ^{126}Sb. Table-1 gives the cumulative/independent yields as well as the corresponding mass yields. The mass yield distribution is plotted figure-1. The mass distribution is a broad Gaussian with a most probable mass of 119.0 ± 0.7 and FWHM of 44.6 ± 0.5 mass units. The total fission cross-section computed from the mass distribution curve is 862mb.

References:

1.S.B.Manohar, A.Goswami, A.V.R.Reddy, B.S.Tomar, P.P.Burte and Satya Prakash Radiochim. Acta 56, 69 (1992)

TABLE-1

Mass yields in 79MeV ^{12}C induced fission ^{232}Th

Nuclide	$r_C(A)$	cumulative cross section	FCY/FIY	r_A
^{91}Sr	5.98 ± 0.65	10.57±1.15	0.96	11.01 ± 1.20
^{92}Sr	5.64 ± 0.42	9.96±0.74	0.90	11.07 ± 0.82
^{95}Zr	8.98 ± 0.64	16.29±1.18	0.98	16.62 ± 1.20
^{97}Zr	10.14 ± 0.44	17.82±0.78	0.89	20.02 ± 0.88
^{99}Mo	16.30 ± 0.46	28.56±0.59	0.99	28.85 ± 0.60
^{101}Mo	12.07 ± 0.18	21.19±0.32	0.95	22.31 ± 0.34
^{103}Ru	13.67 ± 0.33	24.35±0.59	0.99	24.60 ± 0.60
^{104}Tc	13.19 ± 0.39	24.89±0.73	0.99	25.14 ± 0.74
^{105}Ru	13.54 ± 0.72	23.72±1.25	0.98	24.20 ± 1.28
^{107}Rh	16.28 ± 0.64	28.30±1.12	0.98	28.88 ± 1.13
^{112}Pd	17.34 ± 1.12	30.28±1.95	0.87	34.80 ± 2.24
@^{113}Ag	21.36 ± 2.00	37.10±3.47	0.96	38.63 ± 3.62
#^{122}Sb	2.69 ± 0.18*	4.79±0.33	0.14	34.25 ± 2.34
#^{124}Sb	6.81 ± 0.59*	12.64±1.10	0.35	36.12 ± 3.14
#^{126}Sb	6.69 ± 0.67*	13.35±1.36	0.42	31.78 ± 3.24
^{127}Sb	8.40 ± 0.32	14.47±0.55	0.44	32.89 ± 1.25
@^{130}I	6.54 ± 0.24*	11.21±0.41	0.42	26.69 ± 0.98
^{136}Cs	4.79 ± 1.17*	8.13±1.97	0.41	19.84 ± 4.80
^{139}Ba	8.38 ± 0.50	14.11±0.85	0.50	28.22 ± 1.70
^{140}Ba	4.60 ± 0.20	7.16±0.31	0.32	22.37 ± 0.97
^{141}Ce	10.70 ± 0.29	18.41±0.49	0.92	20.01 ± 0.53
^{142}La	4.93 ± 0.26	8.22±0.47	0.40	20.55 ± 1.18
^{143}Ce	9.14 ± 0.32	15.19±0.32	0.67	22.67 ± 0.48
^{147}Nd	3.92 ± 0.18	6.46±0.29	0.81	7.97 ± 0.36
^{153}Sm	3.25 ± 0.22	5.29±0.37	0.64	8.26 ± 0.58

* refers to independent yield.

includes yields of both metastable and ground states.

@ excludes small contribution of β^- decay branching of the isomeric state.

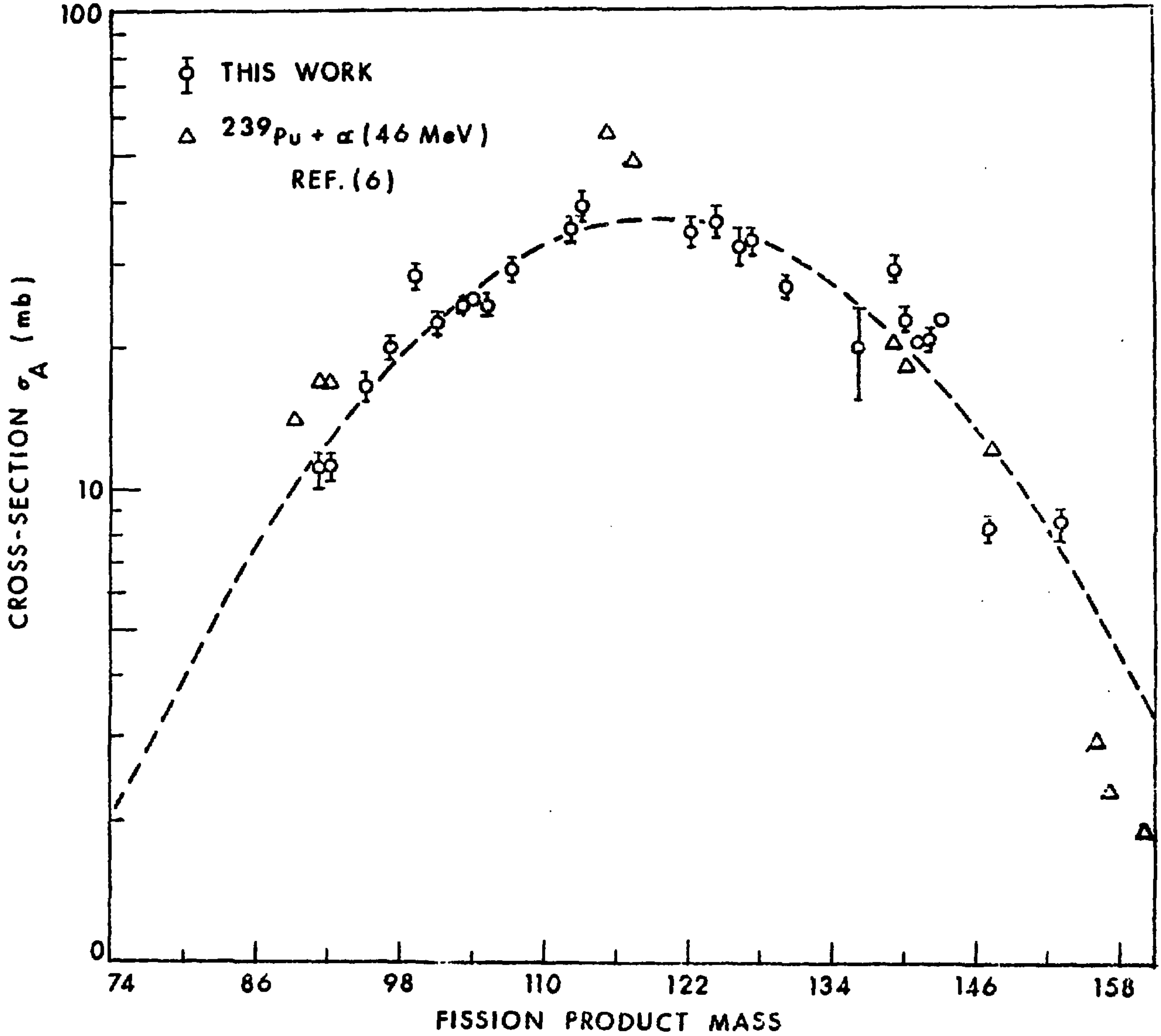
THIS WORK
239Pu + α (46 MeV)
REF. (6)
100
10
0
CROSS-SECTION σA (mb)
74
86
98
110
122
134
146
158
FISSION PRODUCT MASS

Independent Isomeric Yield Ratios of ^{132}Sb in $^{241}Pu(n_{th},f)$ and $^{238}U(\alpha,f)$

B.S.Tomar. A.Goswami. A.V.R.Reddy. S.K.Das.
S.B.Manohar and Satya Prakash
Radiochemistry Division, Bhabha Atomic Research Centre.
Bombay 400 085, INDIA

Independent isomeric yield ratios (IYRs) of ^{132}Sb were determined in $^{241}Pu(n_{th},f)$ and $^{238}U(a,f)$ using fast radiochemical separation followed by gamma spectrometry(1). The corresponding fragment angular momenta were deduced uding standard statistical model code GROGI. Table-1 gives the IYRs and fragments' average angular momenta(J_{av}). Figure 1 shows a plot of fragment angular momenta for ^{132}Sb, ^{130}Sb and ^{128}Sb as a function of excitation energy(Ex) of the fissioning nucleus. The J_{av} in general increases with Ex. However the slope of J_{av} vs Ex is much less for ^{132}Sb than other fragments. This has been explained in terms of the persistence of shell effects even at an excitation energy of about 20 MeV.

References:

1. B.S.Tomar, A.Goswami, A.V.R.Reddy, S.K.Das, S.B.Manohar and Satya Prakash Radiochim. Acta 55, 173 (1991)

2. B.S.Tomar, A.Goswami, S.K.Das, B.K.Srivastava, R.Guin, S.M.Sahakundu and Satya Prakash Phys. Rev. C38, 1787 (1988)

TABLE 1

Fragment angular momenta of ^{132}Sb in
the low and medium energy fission of ^{242}Pu

Fissioning system	Excitation Energy(MeV)	Ym/Ym+Yg)	Average J ($\hbar$)
$^{241}Pu(n_{th},f)$	6.2	0.23 ±0.04	4.62 ± 0.88
$^{238}U(a_{31MeV},f)$	20.5	0.46 ±0.02	7.15 ± 0.34
$^{238}U(a_{38MeV},f)$	27.0	0.44 ±0.06	7.29 ± 1.01

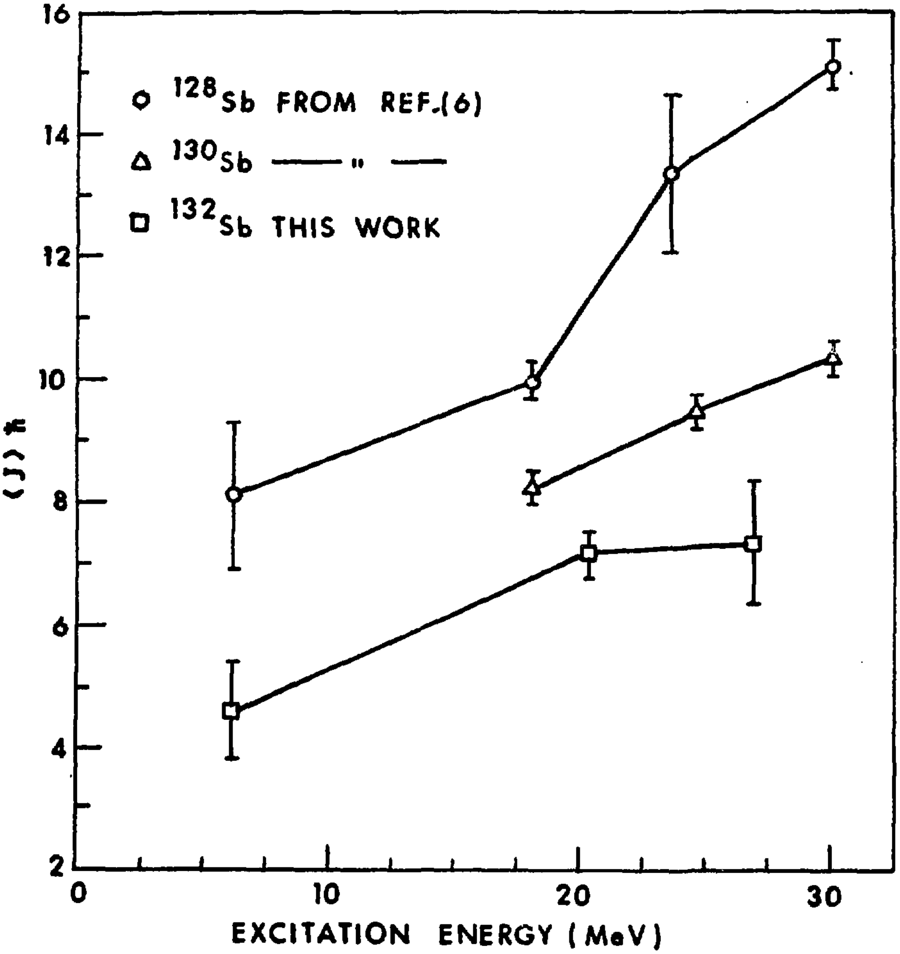

FIG.-2. VARIATION OF FRAGMENT ANGULAR MOMENTUM ⟨J⟩ WITH THE EXCITATION ENERGY OF THE FISSIONING NUCLEUS.

Complete and Incomplete fusion in ^{12}C + ^{93}Nb and ^{16}O + ^{89}Y Reactions

B.S.Tomar, A.Goswami, A.V.R.Reddy, S.K.Das, P.P.Burte,
S.B.Manohar and Satya Prakash
Radiochemistry Division, Bhabha Atomic Research Centre,
Bombay 400 085, INDIA

Excitation functions for the evaporation residues for the reactions ^{12}C + ^{93}Nb and ^{16}O + ^{89}Y in the projectile energy range of 4 to 6.5MeV/amu have been measured using off-line gamma spectrometry(1). The excitation functions for neutron(xn), proton(pxn) and one alpha (axn) emission channels are practically similar for both the reactions. However the products formed by two alpha (2axn) emission show much higher cross sections in the ^{12}C + ^{93}Nb than the ^{16}O+^{89}Y system. This has been explained in terms of the incomplete fusion process involving transfer of an alpha particle from the projectile to the target in the former case.

References:

1. B.S.Tomar, A.Goswami, A.V.R.Reddy, S.K.Das, P.P.Burte, S.B.Manohar and Satya Prakash Z.Phys. A 343, 223 (1992)

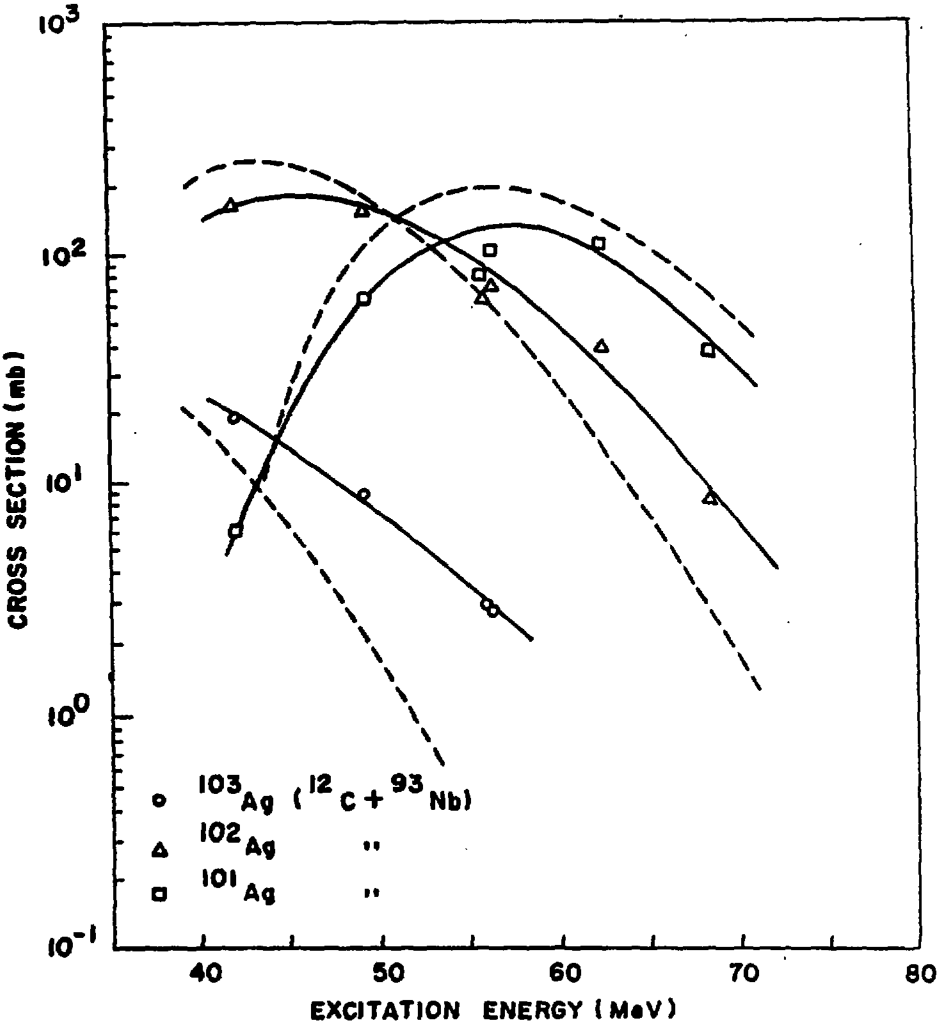

Fig. 1a: Excitation functions for $^{101-103}$Ag isotopes in ^{12}C + ^{93}Nb along with cascade predictions

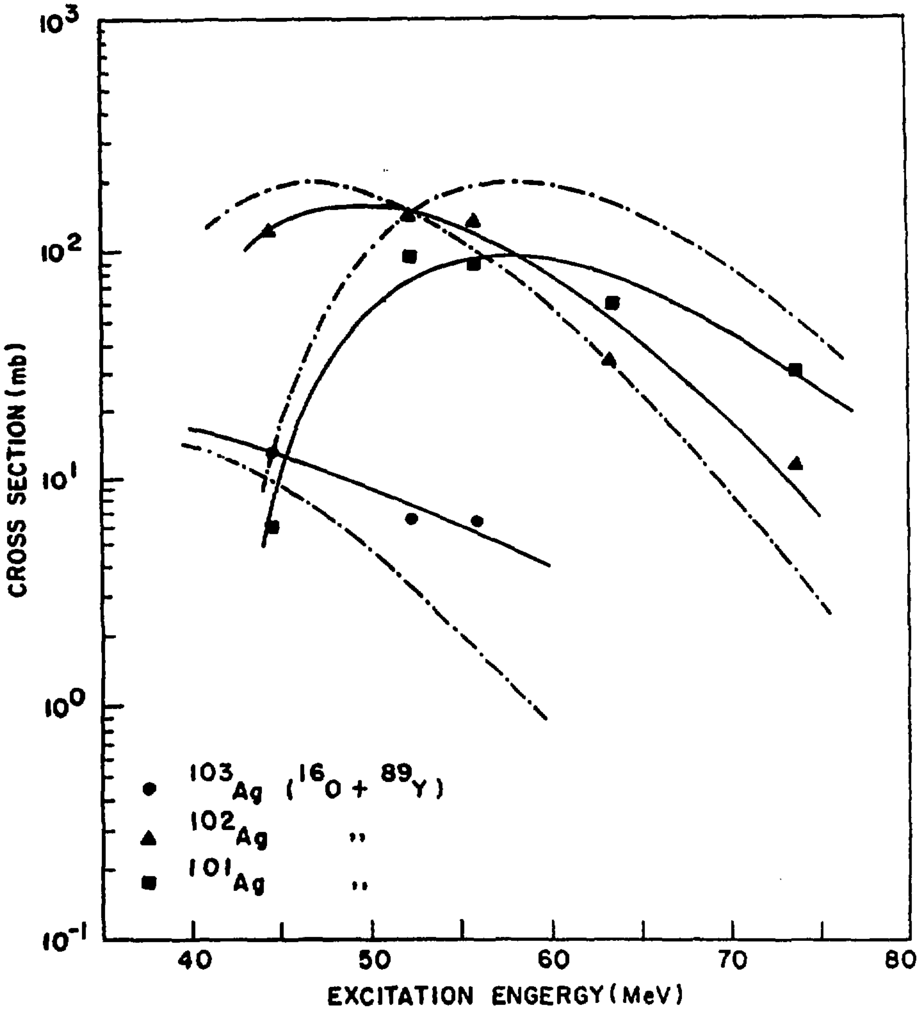

Fig. 1b: Excitation functions for $^{101-103}$Ag isotopes in ^{16}O + ^{89}Y along with cascade predictions

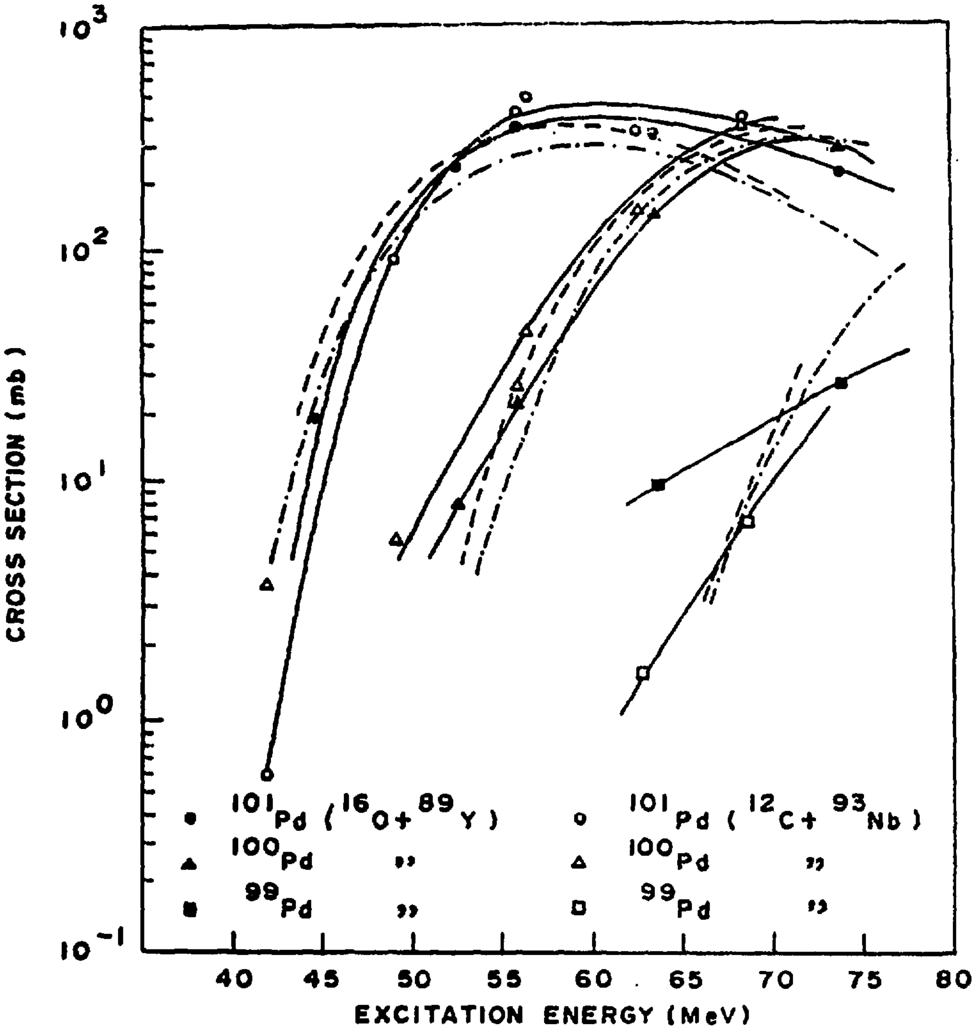

Fig. 2: Excitation functions for $^{99-101}Pd$ isotopes in ^{12}C + ^{93}Nb and ^{16}O + ^{89}Y along with cascade predictions

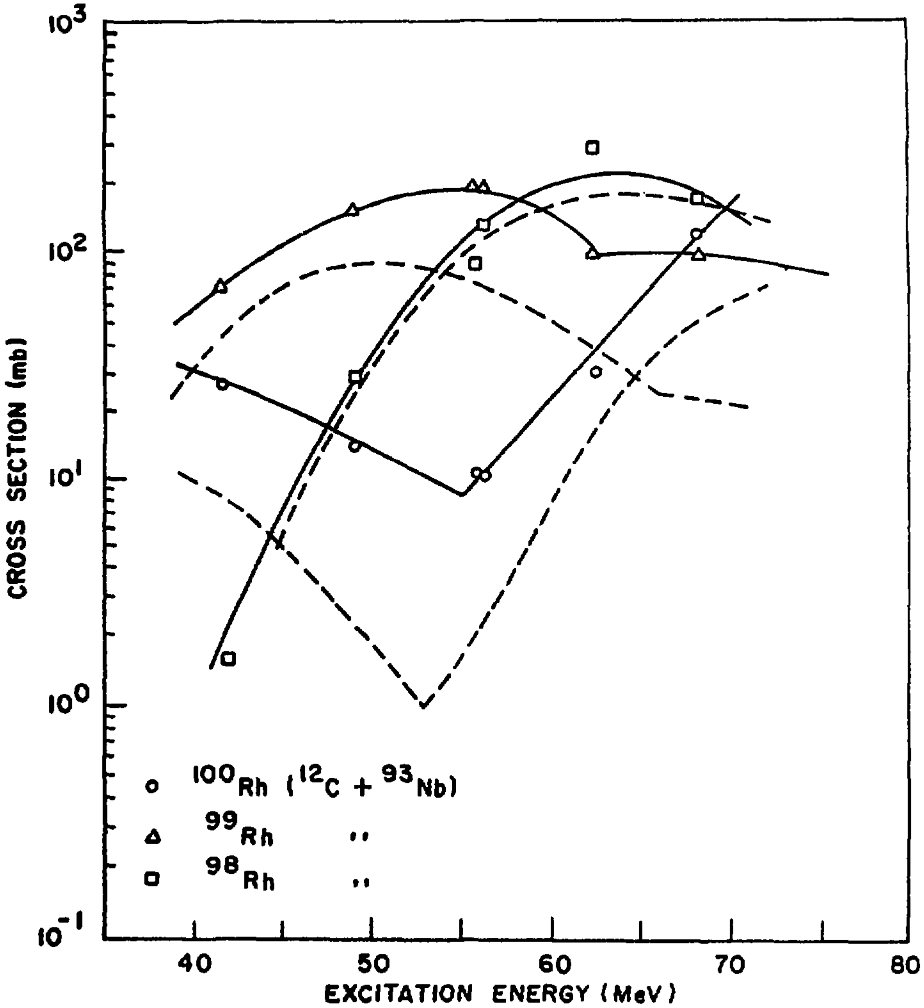

Fig. 3a: Excitation functions for $^{98-100}$Rh isotopes in $^{12}C + ^{93}Nb$ along with cascade predictions

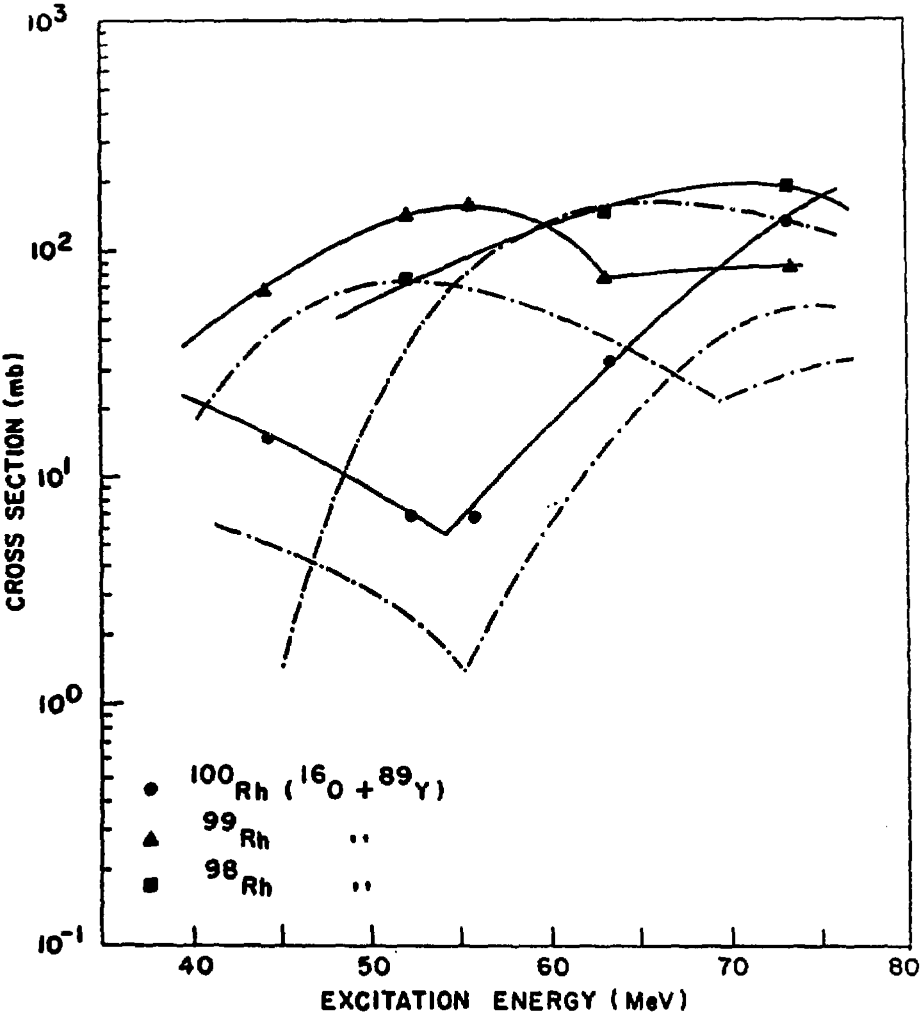

Fig. 3b: Excitation functions for $^{98-100}$Rh isotopes in ^{16}O + ^{89}Y along with cascade predictions

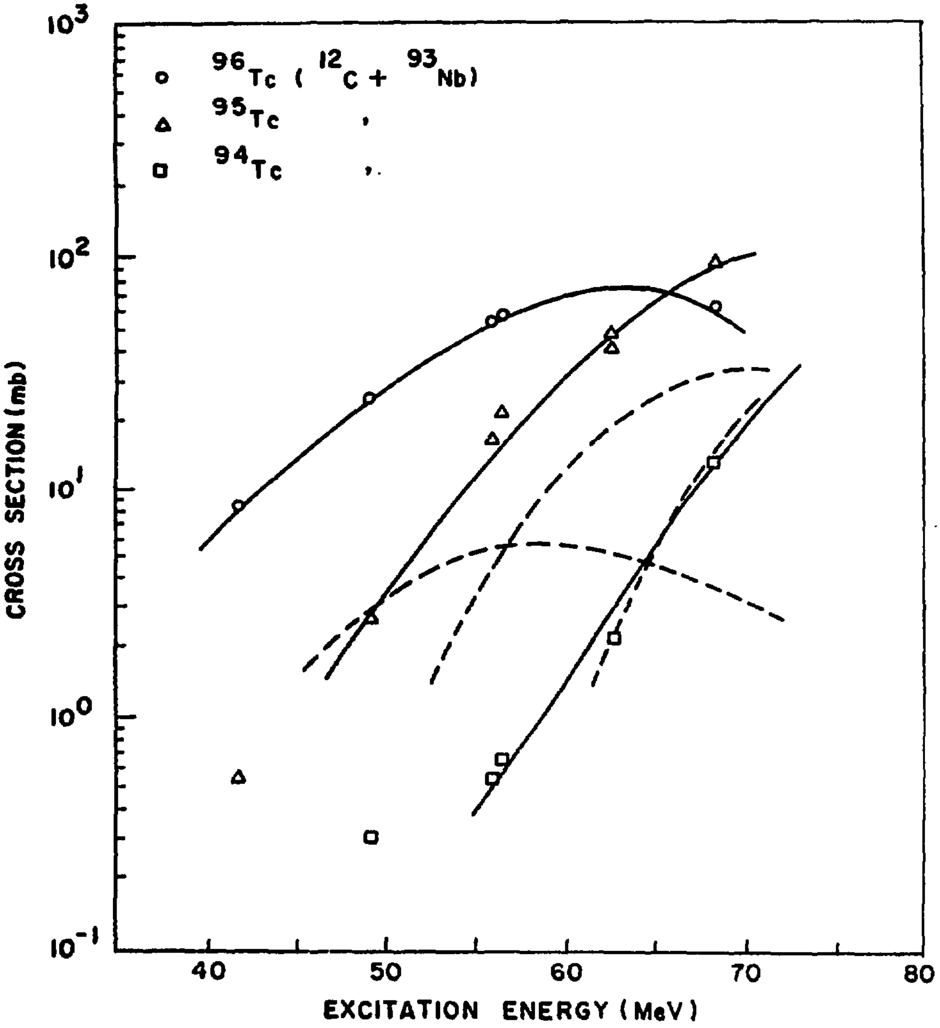

Fig. 4a: Excitation functions for $^{94-96}Tc$ isotopes in ^{12}C + ^{93}Nb along with cascade predictions

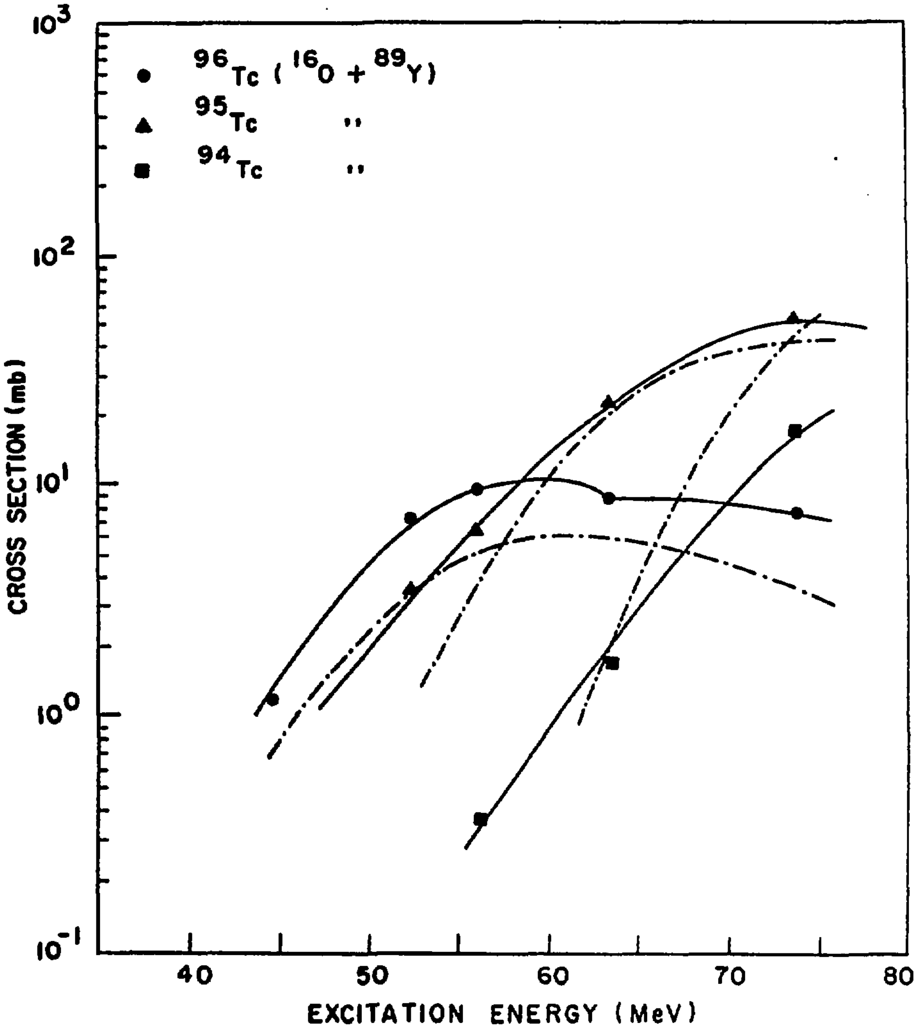

Fig. 4b: Excitation functions for $^{94-96}$Tc isotopes in ^{16}O + ^{89}Y along with cascade predictions

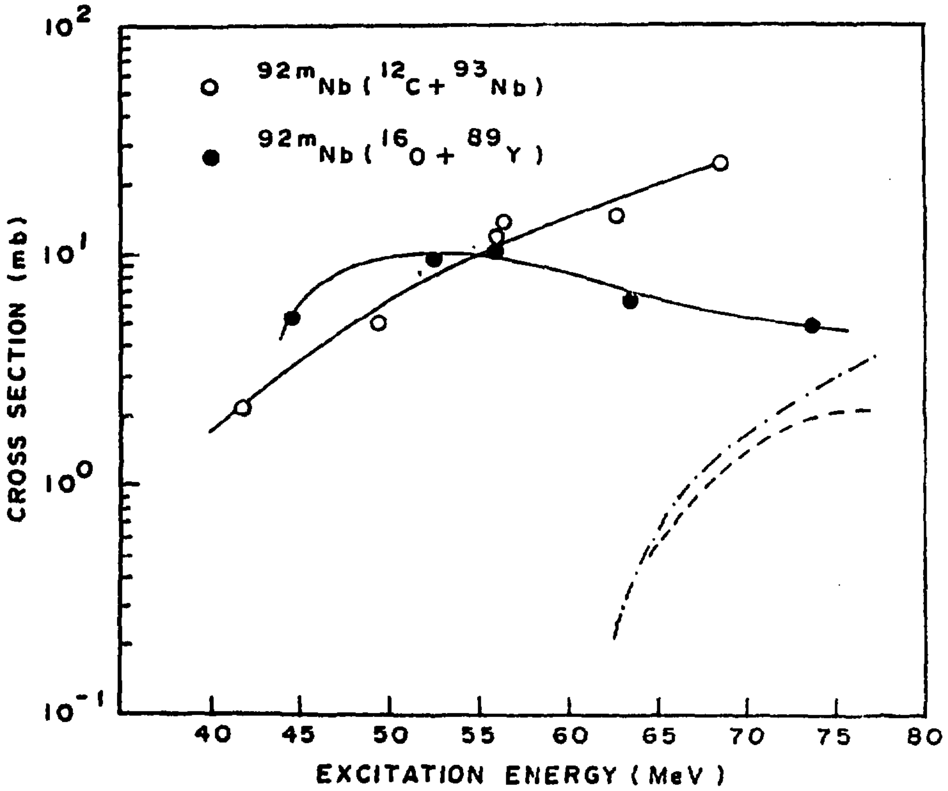

Fig. 5: Excitation functions for ^{92}Nb in ^{12}C + ^{93}Nb and ^{16}O + ^{89}Y along with cascade predictions

Generation of Transport Cross-Section for Hydrogen using B_N-Approximation

R.D.S. Yadav and Vinod Kumar
Theoretical Physics Division
BARC, Bombay - 400 085.

In the analysis of light-water reactor systems, it is very important to take into account the anisotropic nature of scattering Cross-Sections. This is generally done by using appropriate transport Cross-Sections in the place of total cross-sections while solving the transport equation. In the multigroup picture, one can obtain the transport cross-section by using the following expression

$$\sigma_{tr,g} = \sigma_{t,g} - \left(\sum_{g'} \sigma^{1}_{g' \to g} \, J_{g'} \right) / J_g \qquad (1)$$

where,

$\sigma_{tr,g}$ - transport cross-section in group g,

$\sigma_{t,g}$ - total cross-section in gooup g,

$\sigma^{1}_{g' \to g}$ - P_1 Scattering Cross-section from group g' to group g.

J_g - neutron current in the group g.

However, to calculate the transport cross-section from (1) one must know the current spectrum J_g. In reference (1), we discuss the generation of P_N-scattering matrices for hydrogen and solution of B_N equations for a given buckling.

In this manner, we obtain the neutron current spectrum which are then used to find the transport cross-sections from the 69-group WIMS library for hydrogen.

In Table-1,[1] we present the 69-WIMS and our recommended values of transport cross-sections. For further details kindly refer to reference 1.

References :

1. R.D.S.Yadav et al., Generation of Transport Cross-section for Hydrogen using B approximation, Proceedings of the BARC-IGCAR Discussion Meeting, Sept. 1990, BARC.

TABLE - 1

Energy-group structure and recommended transport cross-sections in WIMS-69

Group no:	Upper energy	lower energy	Transport cross-section	
			69-WIMS	Recommended
1	.10000000+08	.60655000+07	1.0655780	1.0655780
2	.60655000+07	.36790000+07	1.1063325	1.3338937
3	.36790000+07	.22310000+07	1.3208651	1.5923044
4	.22310000+07	.13530000+07	1.6357503	1.7528088
5	.13530000+07	.82100000+06	2.1206789	1.8893006
6	.82100000+06	.50000000+06	2.6778705	1.9574760
7	.50000000+06	.30250000+06	3.5906724	2.2188643
8	.30250000+06	.18300000+06	4.3144354	2.3031185
9	.18300000+06	.11100000+06	5.2610499	2.5809887
10	.11100000+06	.67340000+05	6.2107478	2.8869194
11	.67340000+05	.40850000+05	6.8505459	3.2241471
12	.40850000+05	.24780000+05	7.1901462	3.5725232
13	.24780000+05	.15030000+05	7.3040086	3.9244922
14	.15030000+05	.91180000+04	7.2176519	4.2830579
15	.91180000+04	.55300000+04	7.0723300	4.6363266
16	.55300000+04	.35191001+04	6.9418323	4.8845754
17	.35191001+04	.22394500+04	6.9290756	5.1608307
18	.22394500+04	.14251001+04	6.9336614	5.3967613
19	.14251001+04	.90689795+03	6.8097395	5.5922551
20	.90689795+03	.36726196+03	6.7102663	6.1204733
21	.36726196+03	.14872800+03	6.6651149	5.9777331
22	.14872800+03	.75501404+02	6.6526122	5.8151120
23	.75501404+02	.48052002+02	6.6523025	5.9053982
24	.48052002+02	.27699997+02	6.6530284	6.2329080
25	.27699997+02	.15968000+02	6.6872092	6.3320048
26	.15968000+02	.98769999+01	6.7288779	6.3468028
27	.98769999+01	.40000000+01	6.7787806	6.7262283

NEUTRON TRANSPORT CROSS-SECTION FOR HYDROGEN - VALIDATION AGAINST SMALL MULTIPLYING SYSTEMS AND REACTOR SHIELDS

Ashok Kumar and Vinod Kumar
Theoretical Physics Division
Bhabha Atomic Research Centre, Bombay-400085.

The neutron scattering cross-section is highly anisotropic specially with lighter nuclei such as hydrogen. Hydrogen nuclei are abundantly present in light water moderated neutron multiplying systems and reactor shields. Therefore, in order to predict accurately the various parameters of interest for such systems, the anisotropy of scattering must be correctly taken into account while solving the neutron transport equation. Multigroup approach is normally employed to solve the neutron transport equation. In order to save on computing time and other complexities in solving the transport equation, the anisotropy of scattering cross-section upto the Ist order is taken into account by the transport approximation where the total cross-section in each energy group 'g' is replaced by the transport cross-section defined as

$$\sigma_{t_T}^{g} = \sigma_t^{g} - \sum_{g'} \sigma_{s1}^{g' \to g} \; J^{g'} / J^{g}$$

where, σ_{s1} is the first order term in the Legendre Polynomial expansion of the scattering cross-section and J is the neutron current. In the 69-groups WIMS and 16-groups Hansen-Roch multigroup data libraries available with us, the transport cross-sections are obtained by assuming the current spectrum to be Maxwellian in the thermal energy region and varying as 1/E in the fast energy region.

It has been observed that the assumption of current spectrum varying as 1/E is not valid in fast energy range specially for small systems where more number of high energy neutrons leak out of the system before making collisions. For such systems the transport cross-sections are to be determined by correctly employing the current spectrum. These transport cross-sections for hydrogen are calculated by employing the current spectrum obtained by solving the transport equation in fundamental mode for a representative multiplying system. It is shown that using these calculated transport cross-sections for hydrogen the prediction of the results for various critical assemblies and reactor shields improve significantly and are similar to those obtained by employing the anisotropy of scattering exactly upto the first order term.

Investigations Regarding Accuracy of Thorium Cross Sections in WIMS Cross Section Library

P.D. Krishnani
Theoretical Physics Division
Bhabha Atomic Research Centre
Bombay 400 085

The use of thorium in heavy water reactors has been a long standing goal because of its enormous potential to increase energy reserves. This is because of the superior fissile properties of U-233 bred from Th-232 by capturing a neutron and subsequent beta decay. However, very little information exists for lattice physics experiments done with thorium fuel. In this connection, Canadians have performed some integral experiments with ThO2-UO2 fuel in ZED-2 critical facility at Chalk River. They have measured lattice parameters of 19-rod clusters of ThO2 containing 1.5% highly enriched UO2 (having 93% U-235) (1,2). These experiments were done for a range of lattice pitches and with D2O, H2O and air coolants. In another experiment, the measurement of relative conversion ratio was done with 19 rod ThO2 1.45% UO2 fuel in ZED-2 reactor (3).

The above stated experiments of ThO2-UO2 fuel were analysed with the computer code CLUB using WIMS cross section library (6-8). The computer code CLUB (4, 5) is a multigroup integral transport theory code for analysing heavy water moderated lattices. It was found from the analysis of ThO2 experiments that there is a systematic error in the prediction of Keff, which is underpredicted on the average by 1.6% (6). The error in the prediction of Keff for thorium lattices appears very large particularly when it was predicted with 0.5% of unit for UO2 lattices. From this analysis, it was also concluded that the absorption cross section of Th-232 in the thermal range is large. Subsequently we received a communication from Dr. M.J. Halsall (UKAEA) that they have revised data from Th 232. In the revised data of Th-232, it was found that the absorption cross section in the thermal range was indeed less than the old data. The experiments were reanalysed with the new data for Th-232. The Keff was underpredicted by 0.6% with the new data for Th-232 (7). It was concluded that the cross sections for Th-232 may need reevaluation.

References

1. A. Okazaki and S.A. Durrani, AECL 2778, 1967.

2. A. Okazaki, AECL 2779, 1967.

3. R.T. Jones, AECL 5825, 1977.

4. P.D. Krishnani, Ann. nucl.Energy,9, 255, 1982.

5. P.D. Krishnani, Ann. nucl. Energy,9, 287, 1982.

6. P.D. Krishnani, Ann. nucl. Energy 16, 151, 1989.

7. P.D. Krishnani, Ann. nucl. Energy, 16, 659, 1989.

8. P.D. Krishnani et. al., "Analysis of Heavy Water Moderated Lattices Experiments with Thorium Oxide Fuel", Paper presented in Indo Japan Seminar on Thorium Utilization, Dec. 10 13, 1990, Bombay, India.

Nuclear Data Activity During the year 1992

by
V. Jagannathan and R.P. Jain
Theoretical Physics Division
BARC, Bombay - 400 085.

The 1988 version of WIMS-KAERI library which contains 69 group cross section data in thermal reactor applications was received from Dr. S. Ganesan, Nuclear Data Section, IAEA, Vienna. This library was made compatible with the code NEW-MURLI. Reanalysis of all the uniform lattice experimental data on U-metal, UO_2 (enriched), mixed exide (UO_2 + PuO_2) fuel with light water moderators which are available in open literature, was carried out. The new WIMS-KAERI library gives Keff values within $\pm$.0.01 of unity for almost all the cases analysed. The r.m.s. deviation is $< \pm$ 0.005. The old WIMS library which is currently in use shows slightly larger deviations.

INTERNATIONAL CODE INTERCOMPARISON FOR FISSION CROSS-SECTION CALCULATIONS, HAUSER-5 PROGRAM

H.M. Jain and S. Kailas
Bhabha Atomic Research Centre
Bombay 400 085 (India)

For this exercise, we use the HAUSER-5 PROGRAM based on the statistical (Hauser-Feshbach theory with angular momentum and parity conservation) optical model. The neutron transmission coefficients Tl (En) are obtained from the supplied T(l,j) input data, Appendix-1 for Pu-239 and Appendix-2 for Am-241 which are the results of coupled channel calculations. The capture and fission transmission coefficients are calculated as a function of spin and parity J^{π}. The double humped fission barrier model is used for fission calculations. The reaction proceeds in two independent steps :

(i) population of isolated nuclear levels of Class I.

(ii) decay of these levels by neutron, gamma-ray emissions and fissions

The main quantity calculated are the compound nucleus formation cross-sections (σ_c) using the optical model and the competing channels, i.e., compound elastic plus inelastic, capture and fission cross-sections using the statistical model based on the Hausen-Feshbach theory.

The width fluctuation correction is applied to particle channel for discrete level scheme only and not to gamma and fission channels. Tepel et.al method of calculation is used for this correction factor. For the incident neutron energies higher than the last discrete level, such fluctuations are not taken into account. The resonance level interference correction is also not taken into account.

In the present code there is a provision to include upto 100 discrete levels and in the continuum region it uses the Constant temperature and Fermi gas levels formulae. The maximum number of orbital angular momentum and energies for transmission functions and compound nuclear reaction is 32.

Transmission coefficients for gamma ray channels are calculated by assuming E1 (Brink-Axel's formalism-giant dipole resonance model) and M1 (Weiskopf model) transition between all possible existing states, consistent with the appropriate energy and selection rules.

Within the limitations of HAUSER-5 program, applying the usual level densities formulae with an appropriate enhancement factor and using the supplied neutron transmission coefficients, level density parameters, discrete level schemes, fission barriers parameters and fission transition states, we are able to reproduce approximately the energy dependent behaviour of the fission cross section. This program cannot predict the cross sections where no measured data exist, since it needs atleast one value of capture and fission cross section for normalisation. Since there exists no fine structure in fission cross section, the double humped fission barrier is sufficient for these calculations. For this exercise the target nuclei are odd-nuclei $^{239}_{94}Pu^{145}$ and $^{241}_{95}Am^{146}$ and fissioning compound nuclei $^{240}_{94}Pu^{146}$ and $^{242}_{95}Am^{147}$ are even-even and odd-odd respectively. In both these situations the present code does a good job of reproducing the data available and this amply demonstrates the capabilities of HAUSER-5 program for predicting the fission cross sections with reasonable success as shown in Fig.1 and Fig.2 for ^{239}Pu and ^{241}Am respectively.

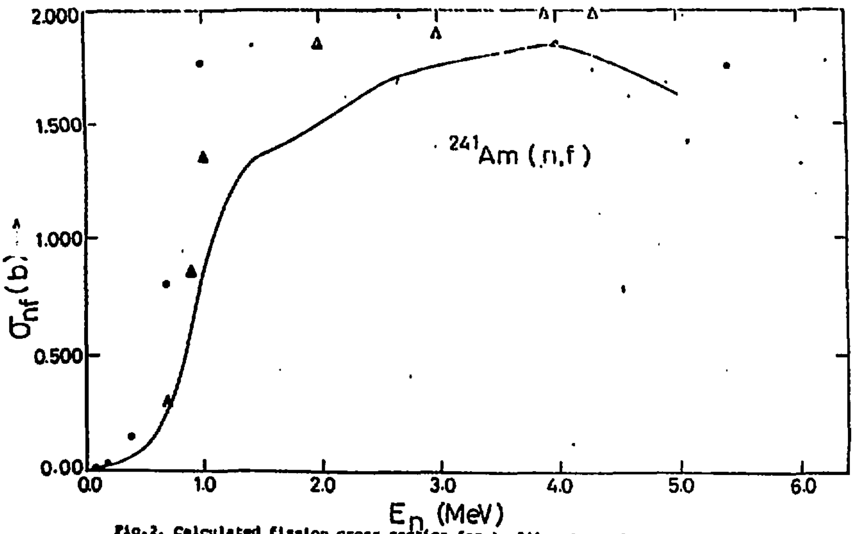

Fig.2. Calculated fission cross section for Am-241.,• JENDL-3
△ Behrens, J.W. UCID-17324 (1976)

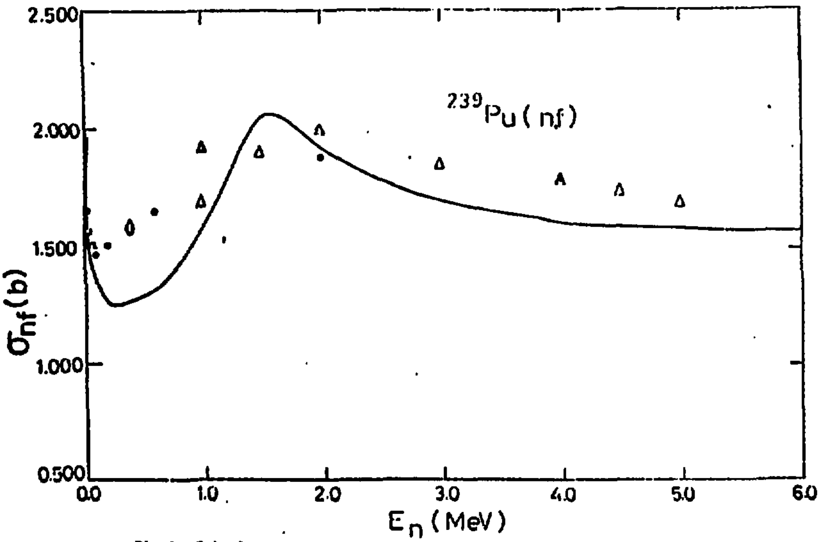

Fig.1. Calculated fission cross section for Pu-239,• JENDL-3
△ Meadows, J.W.; Nucl. Sci. Eng; 68 (1978)360

WIMS LIBRARY UPDATE PROJECT

P. Mohanakrishnan, Reactor Physics Division
IGCAR, Kalpakkam 603 102, Tamil Nadu

1. INTRODUCTION

The 69 energy group WIMS neutron cross section library is one of the most widely used libraries for thermal reactor analysis. IAEA has initiated a WIMS Library Update Project (WLUP) to obtain, in stages, a improved WIMS library from the recently available evaluated data files ENDF/B-VI and JENDL-3.

2. PARTICIPATION IN STAGE-1

As part of the stage-1 of the project, two critical TRX lattices (UO_2/H_2O), three critical BAPL lattices (UO_2/H_2O), three critical ZEEP lattices (UO_2/D_2O) and three exponential BNL lattices (U-233-ThO_2/H_2O) have been analysed [1],[2]. A 1971 version of WIMS library has been used with lattice code MURLI [4] developed in India. The parameters compared are criticality, epithermal to thermal capture ratio in U-238 (ρ^{28}) or thorium (ρ^{02}), ratio of epithermal to thermal fissions in U-235 (δ^{25}), ratio of fissions in U-238 to fissions in U-235 (δ^{28}) and conversion ratio (C). The results are summarised in Table-I. The effects of using hardened fission spectrum and improved σ_{tr} for hydrogen were also investigated [1].

REFERENCES :

1. Mohanakrishnan P., WLUP First Stage Results (Rev-1), RPD/CPOS/34, (1991).

2. Mohanakrishnan P., WLUP Stage-1 Extended Results, RPD/CPOS/58, (1992).

3. Bhatia H.K., Private Communication inBARC (1976).

4. Huria H.C., Atomkernenegie <u>31</u>, 87 (1978).

Table-I

Comparison of Calculation and (Experiment) when 1971 Version of WIMS Library is Used

Benchmark	Keff	ρ^{28}(U lattices) or ρ^{02}(Th lattices)	δ^{25}	δ^{28}	Conversion Ratio(C*) or Relative Conversion Ratio (RCR)
TRX-1	1.0028	1.300 (1.320 ± 0.021)	0.0989 (0.0987 ± 0.001)	0.0897 (0.0946 ± 0.0041)	0.789 (0.797 ± 0.008)
TRX-2	0.9992	0.815 (0.837 ± 0.016)	0.0608 (0.0614 ± 0.0008)	0.0642 (0.0693 ± 0.0035)	0.640 (0.647 ± 0.006)
BAPL-1	0.9975	1.409 (1.39 ± 0.01)	0.0844 (0.084 ± 0.002)	0.0714 (0.078 ± 0.004)	- -
BAPL-2	0.9977	1.17 (1.12 ± 0.01)	0.0689 (0.068 ± 0.001)	0.0616 (0.070 ± 0.004)	- -
BAPL-3	0.9975	0.920 (0.906 ± 0.01)	0.0529 (0.052 ± 0.001)	0.0507 (0.057 ± 0.003)	- -
ZEEP-1	0.9933	- -	- -	0.0668 (0.0675 ± 0.0014)	1.272 (1.260 ± 0.005)
ZEEP-2	1.0026	- -	- -	- -	- -
ZEEP-3	1.0081	- -	- -	- -	- -
BNL-1	0.9820	1.334 (1.338± 0.042)	- -	- -	- -
BNL-2	0.9881	0.921 (0.903 ± 0.038)	- -	- -	- -
BNL-3	1.0007	0.424 (0.421 ± 0.013)	- -	- -	- -

Disc : MISC-I
File : PM1

Radiative Capture Cross Sections for Mercury-202

V. Gopalakrishnan

Reactor Physics Division, IGCAR, Kalpakkam 603102.

Capture of a neutron by 80-Hg-202, a stable isotope of Mercury (abundance 29.8%), results in Hg-203, a radioactive nuclide with a half life of roughly 47 days. When the Hg-203 was suspected to have been drawn from a manometer into the FBTR core, the (n, γ) cross sections of Hg-202 were required to estimate the amount of mercury drawn into the reactor. Since the nuclide sees the spectrum of reactor neutrons, the cross sections in the entire energy region of reactor neutrons are needed. On scanning several of the literature dealing with neutron cross sections and also the basic neutron cross section libraries available with us, an evaluation for Hg-202 was not found. In order to meet the requirement, reconstruction of smooth cross sections over energies varying from sub-thermal to 20 MeV was made. The neutron cross section document BNL-325/1/ and the paper by Beer and Macklin/2/ (which happened to be the latest data in EXFOR received from IAEA), were the data sources for this work. The details of this work and the (n,γ) cross sections constructed are presented in an internal note /3/.

It is to be noted that ACTL-82 evaluation/4/, received from IAEA after the completion of this work, gives cross sections for Hg-202 differing considerably from ref. 1 and 2.

1. S. F. Mughabghab and G. I. Garbar, Neutron Cross Sections, BNL-325 (1973).

2. H. Beer and R. L. Macklin, Phys. Rev./C, 32, p.738 (1985).

3. V. Gopalakrishnan, Radiative Capture Cross sections of Mercury-202, Internal Note RPD/NDS/39 (1990).

4. H.D.Lemmel, ACTL-82: The LLNL Evaluated Neutron Activation Cross Section Library of 1982, IAEA-NDS-55 (1983).

Towards Recommending a Cross Section Set For PFBR Analysis

K. Devan, V. Gopalakrishnan and S. M. Lee

Reactor Physics Division, IGCAR, Kalpakkam 603102.

Most of the LMFBR core physics neutronics calculations at IGCAR make use of the Cadarache Version 2 set/1/. But, this set was found inadequate for the detailed analysis of PFBR because it overpredicts the k-eff by about 3% of (i) the 1200 MWe theoretical benchmark/2/ in comparison with that predicted by BNAB-78 (adjusted Russian) and CARNAVAL-IV (adjusted French) sets and (ii) the 500 MWe benchmark/3/ in comparison with that predicted by BNAB-78 set and also because of the economic penalties associated with such an uncertainty. It should be noted that CARNAVAL-IV and BNAB-78 sets (not available in India) are recognised to be reliable for fast reactor calculations. It is thus realised that a better cross section set than the existing Cadarache Version 2 set is required for PFBR analysis.

Our earlier critical assembly analyses/4/ showed that the first version of our JENDL-2 based cross section set/5/ was better than Cadarache set for big reactors. Further analysis/6/ showed that it agreed well with the CARNAVAL-IV and BNAB-78 sets in predicting keff of the 1200 MWe benchmark. However, it must be noted that the fission spectrum adapted in this first version was from the Cadarache Version 2 set. Hence, towards recommending a cross section set for PFBR analyses we have two options at present: (i) to make the JENDL-2 based set self-consistent by incorporating suitably averaged fission spectrum from JENDL-2 itself and (ii) to improve the Cadarache set.

(i) Adapting JENDL-2 fission spectrum: The structure of the Cadarache Version 2 set, which we adhere to, allows only one representative fission spectrum for the entire set. A study/7/ was performed to obtain average multigroup fission spectrum weighted with various realistic cases of atom densities and flux shapes, starting from the basic data on fission neutron energy distribution given in the JENDL-2 library, and to see its effect on keff. This study gave rise to a fission spectrum consistent with our JENDL-2 based set, suitable for our PFBR calculations.

(ii) Improving Cadarache Version 2: From a detailed study/6/ of reaction rate integrals of 1200 MWe benchmark, it was found that Cr, Ni and Mn capture rates calculated with Cadarache set were almost double, and Pu-241 fission rate was 19.6% higher than the corresponding values obtained with JENDL-2 set. These materials were replaced in Cadarache set from JENDL-2 set, individually or in combination, and at each stage, the k-eff prediction is as in Table 1. From Table 1 it is found that Cadarache Version 2 set with Pu-241 replaced from JENDL-2 set gives k-eff closest to the desired CARNAVAL-IV value. Since Pu-241 data was not involved in the cross section adjustment that led to the Cadarache Version 2 set, it appears permissible to replace it with a newer data.

Table 1. Comparison of k-eff's calculated with Cadarache Version-2 set in which some materials are replaced from JENDL-2 set.

No.	Materials replaced	k-eff	pcm deviation *
1.	No material replaced	1.04294	+3024
2.	Cr, Ni, Mn	1.03744	+2474
3.	Pu-241	1.01360	+90
4.	Cr, Ni, Mn, Pu-241	1.00818	-452
5.	Ni, Pu-241	1.00994	-276
6.	Cr, Ni, Mn, Pu-240, Pu-241	1.01033	-137
7.	Cr, Ni, Mn, U-238, Pu-241	1.00336	-934
8.	Cr, Ni, Mn, U-238, Pu-240, Pu-241	1.00553	-717

* w.r.t. reported CARNAVAL-IV result, giving keff = 1.01270

This study resulted in the recommendation of either the JENDL-2 based set with consistent fission spectrum or the Cadarache Version 2 set with Pu-241 replaced from JENDL-2. The latter being an adjusted set, may have an edge over the former.

1. J. Ravier, Sections Efficaces Multigroupes et Jeu SEPR a 25 Groupes, CEN de Cadarache, Internal Report PNR/SEPR-66-050 (1966).

2. L. G . LeSage, et al., Proc. NEACRP/IAEA spl. Mtg. on International Comparison Calculation of a Large Sodium-Cooled Fast Breeded Reactor, ANL, Feb 1978, Report ANL-80-78 (August 1980).

3. P. V. K. Menon and P. Mohanakrishnan, Benchmark Model of a Medium Sized FBR for Core Physics Analysis, Internal Note, RPD/CPOS/09.

4. K. Devan, V. Gopalakrishnan, M. M. Ramanadhan and S. M. Lee, Analyses of Selected Fast Critical Assemblies Using JENDL-2 Based Unadjusted Multigroup Data, IGC Report, IGC-124(1991).

5. V. Gopalakrishnan, M.M. Ramanadhan, K. Devan and S. Ganesan, Multigroup Cross Sections from JENDL-2 Point Data File, Internal Note RPD/NDS/42 (1991).

6. K. Devan, V. Gopalakrishnan and S. M. Lee, FBR Benchmark Analysis Towards Recommending A Cross Section Set for PFBR Core Physics Calculations, IGC Report IGC-134 (1992).

7 V. Gopalakrishnan, K. Devan and S.M. Lee, Fission Spectrum for the JENDL-2 Based Cross section Set, Internal Note RPD/NDS/48 (1992).

Calculation of Fission Spectrum from JENDL-2

V. Gopalakrishnan and S. M. Lee

Reactor Physics Division, IGCAR, Kalpakkam 603102.

Recently, a complete multigroup cross section set (Unadjusted) with 31 materials was created from the Japanese Evaluated Nuclear Data File (JENDL-2) in the same form as the adjusted Cadarache Version 2 Set/1/. Even though the group average values of fission spectra (χ) depend on the fissionable nuclides, their atom densities and flux shape in a given reactor, the adjusted Cadarache set gives a common (or representative) fission spectrum to be used for the neutronic calculation of any reactor. This in principle may not be serious because the cross sections have been adjusted adequately. On the contrary, in an unadjusted set, there is no unique way of defining a common multigroup fission spectrum that would satisfy a variety of fast reactors. Therefore, the fission spectrum of Cadarache set was adapted in the first version of our JENDL-2 based cross section set/2/ referred above, and analyses/3,4/ of several benchmark criticals showed its performance to be fair. However, one would prefer, for consistency and completeness, to have the fission spectrum also from JENDL-2 in this set. Hence a study was taken up towards arriving at a common fission spectra to satisfy at least the need of fast power reactor analysis, for which our JENDL-2 based cross sections seem reasonably good.

In JENDL-2 (as in any other ENDF type file), the fission neutron energy distribution $\chi^i(E'\to E)$ for each fissionable nuclide i is given in one of several representations, but mostly in the simple Maxwellian form, where E' is the incident energy, E the fission neutron energy. The multigroup fission spectrum for the neutronic calculations must be averaged as

$$\chi^i_g = \int_{E'}\int_{E\in g} \chi^i(E'\to E)\,\nu^i(E')\,\sigma^i_f(E')\,\phi(E')\,dE\,dE' \Big/ \int_{E'} \nu^i(E')\,\sigma^i_f(E')\,\phi(E')\,dE'$$

But, taking advantage of the weak dependence of χ on E', we assume

$$\chi^i_g = \int_{E\in g} \chi^i(E'\to E)\,dE$$

Using the above method, χ_g were calculated for Th-232, U-233, U-235, U-238, Pu-239, Pu-240, Pu-241 and Pu-242 in 25 groups, corresponding to $E' = 100$ keV. The combined fission spectrum was then computed as

$$\chi^C_g = \sum_i a_i\,\chi^i_g \sum_{g'} \langle\nu\sigma_f\rangle^i_{g'}\,\phi_{g'} \Big/ \sum_i a_i \sum_{g'} \langle\nu\sigma_f\rangle^i_{g'}\,\phi_{g'}$$

where a_i are the atom densities in a given region of a reactor and $\phi_{g'}$ the neutron flux. Representative averge fission spectra obtained by weighting with various cases of atom densities and flux shapes were used in the analysis of the 1200 MWe (Theoretical) benchmark and the observations are documented in an internal note/5/.

1. J.Ravier, Section Efficaces Multigroupes et Jeu SEPR a 25 Groupes, CEN de Cadarache, Internal Report PNR/SEPR-66-050 (1966)

2. V. Gopalakrishnan, M.M. Ramanadhan, K. Devan and S. Ganesan, Multigroup Cross Sections from JENDL-2 Point Data File, Internal Note RPD/NDS/42 (1991).

3. K. Devan, V. Gopalakrishnan, M. M. Ramanadhan and S. M. Lee, Analyses of Selected Fast Critical Assemblies Using JENDL-2 Based Unadjusted Multigroup Data, IGC Report, IGC-124(1991).

4. K. Devan, V. Gopalakrishnan and S. M. Lee, FBR Benchmark Analysis Towards Recommending A Cross Section Set for PFBR Core Physics Calculations, IGC Report IGC-134 (1992).

5. V. Gopalakrishnan, K. Devan and S.M. Lee, Fission Spectrum for the JENDL-2 Based Cross section Set, Internal Note RPD/NDS/48 (1992).

Multigroup Cross sections from ENDF/B-VI

V. Gopalakrishnan and S. M. Lee

Reactor Physics Division, IGCAR, Kalpakkam 603102.

It was decided to add to the Cadarache Version 2 Multigroup cross section data set, available in our division, unshielded multigroup cross section data for some materials not present but which are occasionally required for reactor analysis. The chosen materials, were Li-6, Li-7, Mg, Ti, V, isotopes of Eu Gd, Sb, Am-241, Pa-231, Pa-233, U-232, U-237, Np-238 and Pu-38. The basic data file ENDF/B-VI obtained recently from IAEA, that contained all the above materials was chosen for the purpose. By using IAEA processing codes/1/ LINEAR and RECENT for reconstructing the ENDF data into linearly interpolable point data and by using our code REX1-87/2/, multigroup cross sections, and scattering transfer matrices were calculated. Since ENDF/B-VI, unlike the other versions, does not explicitly give $\bar{\mu}(E)$ (Average cosine of scattering angle in the Lab system), that is involved in the definition of transport cross section, $\bar{\mu}(E)$ were calculated from the data on SNAD (Secondary Neutron Angular Distribution, by a new program AMUL4/3/ written here for the purpose. The unshielded (infinite dilution) multigroup cross sections computed by REX1-87 for these materials were added to the Cadarache data set in binary by a program ADREX1/4/.

1. D. E. Cullen, Summary of ENDF/B Preprocessing Codes, IAEA-NDS-39, Rev. 3.

2. V. Gopalakrishnan and S. Ganesan, REX1-87 - A Code for Multigrouping Neutron Cross sections from Preprocessed ENDF/B Basic Data File, Internal Note RPD/NDS/13 (1988)

3. V. Gopalakrishnan, AMUL-4: A Program to Calculate Average Cosine of Elastic Scattering Angle in the Laboratory System from the Data on Angular Distributions, IGC Report, IGC-141 (1992).

4. V. Gopalakrishnan, ADREX1 - A Program to add unshielded multigroup cross sections to Cadarache Version 2 Cross Section Set Directly from REX1 Output, unpublished.

Calculation of Average Cosine of Elastic Scattering Angle

V. Gopalakrishnan

Reactor Physics Division, IGCAR, Kalpakkam 603102.

Average cosine $\bar{\mu}(E)$ of the elastic scattering angle in the laboratory system is involved in the definition of the transport cross section. This quantity has been explicitly given in the ENDF/B upto its fifth version (ENDF/B-V) and is not given in the ENDF/B-VI. Since we took up processing and multigrouping of some materials from ENDF/B-VI, it was necessary to derive this from the Secondary Neutron Angular Distribution (SNAD) given in ENDF/B-VI. A program AMUL-4/1/ was written for this purpose, that works on the simple kinematic relations, and the usual methods of Legendre expansion of the elastic scattering. The program was validated by computing $\bar{\mu}$ from ENDF/B-IV SNAD data and comparing it with those given explicitly in the same evaluation. Very good agreement was obtained for most of the materials tested and at most of the enegies, even though significant differences were noticed for some light nuclides at a few energies, probably due to inconsistencies between SNAD and $\bar{\mu}(E)$ in ENDF/B-IV. This program was used to obtain $\bar{\mu}(E)$ for the materials chosen for multigrouping from ENDF/B-VI basic data file, obtained recently from IAEA.

1. V. Gopalakrishnan, AMUL-4: A Program to Calculate Average Cosine of Elastic Scattering Angle in the Laboratory System from the Data on Angular Distributions, IGC Report IGC-141 (1992).

Unshielded Multigroup Cross Sections of Major Fission Products from ENDF/B-VI

K. Devan and V. Gopalakrishnan

Reactor Physics Division, IGCAR, Kalpakkam 603 102

At IGCAR, an unadjusted multigroup cross section set has been created/1/, based on the Japanese Evaluated Nuclear Data File Version 2 (JENDL-2) in the same format as the Cadarache Version 2 data extensively used in our Division. Our analyses have shown that this JENDL-2 based set is superior to the Cadarache Version 2 set in keff predictions for fast power reactors like PFBR. In order to add, to this set, multigroup data for the fission products, suitably lumped, we have chosen the most recent American Evaluated Nuclear Data File Version 6 (ENDF/B-VI). Based on recommendations in literature, we have selected some 112 fission product nuclides, from this library. The data have been preprocessed and the cross sections reconstructed to obtain linearly interpolable point data, from the non-linear point data and resonance parameters, using IAEA preprocessing codes. From the reconstructed point data, unshielded *multigroup cross sections including elastic-inelastic* transfer matrices have been obtained. Since ENDF/B-VI does not give the elastic scattering angle cosine ($\bar{\mu}$), required to define transport cross sections, the code AMUL4/2/ was employed to obtain $\bar{\mu}$ from the data on secondary neutron angular distributions (SNAD). Preparation of the lumped fission product data suitable for our requirement is under way.

1. V. Gopalakrishnan et al., Multigroup Cross Sections from JENDL-2 Point Data File, Internal Note RPD/NDS/42 (1991).

2. V. Gopalakrishnan, AMUL-4: A Program to Calculate Average Cosine of Elastic Scattering Angle in the Laboratory System from the Data on Angular Distributions, IGC Report, IGC-141 (1992).

Expansion of the Cadarache Version 2 Multigroup Cross section Set

V. Gopalakrishnan

Reactor Physics Division, IGCAR, Kalpakkam 603 102

Our analysis/1/ has shown that the Cadarache Version 2 Cross section Set which overpredicts the keff of a fast power reactor like PFBR (by about 3%, compared to that predicted by CARNAVAL-IV) becomes as good as the recent adjusted French or Russian sets viz. CARNAVAL-IV and BNAB-78 respectively, when data of some nuclides, Pu-241 for instance, is replaced from our JENDL-2 based set/2/. However, it does not include data for nuclides required at times. For instance, it does not contain data for several higher actinides required for studies on the actinide buildup with burnup and the consequences. It does not include data for Antimony, which is a neutron source at startup of FBTR. In view of all the above, an extended data set was created as follows:

1. All the data (38 materials) of Cadarache Version 2 set retained.

2. Data for Fe, Cr, Ni, Mo and Pu-241 added from our JENDL-2 based set.

3. Data for Sb-121 and Sb-123 added from ENDF/B-IV

4. Data for higher actinides, not covered already, are taken from ENDL/84-V.

For the present self shielding is not considered for the data mentioned in 3 and 4 above. A card-image version of the above has been created on a magnetic tape and the binary version is already in use on the ND-570 computer system.

1. K. Devan et al., FBR Benchmark Analyses Towards Recommending a Cross section Set for the PFBR Core Physics Calculations, Report IGC-134 (1992).

2. V. Gopalakrishnan et al., Multigroup Cross Sections from JENDL-2 Point Data File, Internal Note RPD/NDS/42 (1991).

Average Delayed Neutron Fractions from ENDF/B-VI

V.Gopalakrishnan and P.Mohanakrishnan

Reactor Physics Division, IGCAR, Kalpakkam 603 102

The importance of the delayed neutrons is well known in the context of control of a fission reactor. Efforts on the improvement of the data on the delayed neutron yield, its dependence on the incident neutron energy and the temporal groups, its energy distribution (spectrum), etc. are continually made at leading institutions of the world, both by experimental and theoretical means, resulting in revisions of the delayed neutron data in the basic evaluated nuclear data files. Motivated by the publication of the recent evaluation of delayed neutron data by Brady and England/1/, part of which was supposed to be included in the American Evaluated Nuclear Data File Version 6 (ENDF/B-VI), we calculated the average delayed neutron fractions for various fissionable nuclides of importance from the ENDF/B-VI, most recently (1991) obtained from IAEA. On comparison, we find the absolute yield of delayed neutrons per fission, taken from ENDF/B-VI library, coincide with the older values of ENDF/B-V, though the calculated values published by Brady and England/1/ differ considerably from the older ones. An internal note/2/ has been written to record the observations. A comparison of the average absolute delayed neutron yields is given Table 1.

1. Brady and England, Nucl. Sci. Engg. 103 (1989) p.129.

2. V. Gopalakrishnan and P. Mohanakrishnan, Average Delayed Neutron Fractions from ENDF/B-VI, Internal Note RPD/NDS/50 (1992).

Table 1

Comparison of Total Delayed Neutron Yield per Fission

Nuclide	Brady	ENDF/B-V	ENDF/B-VI
Th-232	0.0564	0.0527	0.0527
U-233	0.0097	0.0074	0.0074
U-235	0.0178	0.0167	0.0167
U-238	0.0405	0.0440	0.0440
Pu-239	0.0076	0.0065	0.0065
Pu-240	0.0081	0.0090	0.0090
Pu-241	0.0141	0.0162	0.0162
Pu-242	0.0143	0.0197	0.0197

Calculation of Helium Produced in Stainless Steel due to Neutron Irradiation

V. Gopalakrishnan

Reactor Physics Division, IGCAR, Kalpakkam 603 102

To get an idea of how well a sophisticated experimental determination of the helium produced in stainless steel due to neutron irradiation, agree with a theoretical estimation taking into account all available information, a study was earlier made/1/ for two austenitic steel samples with which Nandedkar and Kesternich/2/ have made measurements and reported. Our calculations accounted for the helium production due to (n,alpha) reactions in all the components of the specimens and also due to the two step process viz. Ni-58(n,gamma)Ni-59(n,alpha)Fe-56, which accounts for the majority of the helium produced at high fluences. At that time KEDAK-4 (German) was the only nuclear data library, available with us, giving data for Ni-59. Now, the most recent American Evaluated Nuclear Data File Version 6 (ENDF/B-VI) includes data for this nuclide, and hence the entire exercise was repeated with this new data. Even though the results with the newer data tend to approach the experimental values, disagreement of over a factor of two remain as seen in Table 1. Closer observation has shown that uncertainties in the measurement as well as in the data must be responsible for this difference.

1. V. Gopalakrishnan et al., Estimation of Helium Production in Stainless Steel due to Neutron Irradiation, in Proc. DAE Symp. Nucl Phys., Aligarh Muslim University, Aligarh, Dec 26-30, 1989.

2. R. V. Nandedkar and W. Kesternich, J. Nucl. Matr., 62 (1989) 329.

Table 1

Comparison of Calculated and measured values of helium produced (in atom parts per million, appm)

Sample	Measured	Ref. 1	Present
1.4970	70	132	124
1.4970LB	28	94	80

Calculation of Multigroup Displacement Damage Cross Sections

S.Selvi, V. Gopalakrishnan and M.M. Ramanathan

Reactor Physics Division, IGCAR, Kalpakkam 603 102

Displacement damage cross sections are required for the study of changes in the mechanical properties of structural materials in the radiation environment in fission or fusion systems. 25 group (Cadarache Version 2 structure) damage cross sections were calculated from (i) the RECOIL data base, using program RECOIL, and also from (ii) the SPECTER data base using program SPECTER.

(i) The RECOIL System

The RECOIL data base/1/ consists mainly of recoil spectrum of the primary knock on atoms (PKA) in 105 neutron groups and 104 recoil groups, derived mainly from ENDF/B-IV, for neutron reactions significant for radiation damage studies. The original RECOIL program could calculate the damage cross section of a single element or an alloy of materials (for which data is available in the RECOIL Data Base). However, it did not have provision to obtain broad group damage cross sections. The code was modified to include a subroutine to calculate broad group cross sections from the 105 group data using an input weighting spectrum. The modified program was used to obtain 25 group damage cross sections/2/ for the following nuclides:

The numbers in brackets refer to the ENDF MAT numbers.

Li-6(1271),	Li-7(1272),	Be(1289),	B-10(1273),	B-11(1160),
C(1274),	N(1275),	O(1276),	Mg(1280),	Al(1193),
Si(1194),	Ti(1286),	V(1196),	Cr(11910,	Mn(1197),
Fe(1192),	Co(1199),	Ni(1190),	Cu(1295),	Zr(1284),
Nb(1189),	Mo(1287),	Ta-181(1285),	Ta-182(1127),	W(1128),
Au(1283),	Pb(1288).			

(ii) The SPECTER System

The source for SPECTER data base/3/ was mainly ENDF/B-V with some data from ENDF/B-IV. The SPECTER data base mainly consists of 100 group cross sections for reactions essentially involved in radiation damage. The SPECTER code can calculate the total damage cross section, for a given nuclide or a mixture, in a given group structure, and also the dpa (number of displacements per atom) for a given fluence. Since we found the code to do multigroup collapsing from the 100 group structure to a given broader group structure, with only flat (energy independent) weighting, we modified the code to apply flux weighting. With the modified code we calculated/4/ the total damage cross sections for all the 41 nuclides in the data base, given below:

H(1301),	He-3(1146),	He-4(1270),	Li-6(1303),	Li-7(1272),
Be(1304),	B-10(1305),	B-11(1160),	C (1306),	N (1275),
O (1276),	F (1309),	Na(1311),	Mg(1312),	Al(1313),
Si(1314),	P (1315),	S (1316),	Cl(1149),	K (1150),
Ca(1320),	Ti(1322),	V (1323),	Cr(1324),	Mn(1325),
Fe(1326),	Co(1327),	Ni(1328),	Cu(1329),	Zr(1340),
Nb(1189),	Mo(1321),	Ag-107(1371),	Ag-109(1373)	Ta (1285),
W-182(1128),	W-183(1129),	W-184(1130),	W-186(1131),	Au (1379),
Pb(1382)				

1. T.A.Gabriel., J.D.Amburgey and N.M.Greene, Radiation Damage calculations : Primary Recoil Spectra, Diplacement Rates, and Gas - production Rates, Report ORNL/TM/5160 (1976).

2. S.Selvi,M.M Ramanathan,V.Gopalakrishnan , 25 Group Damage Cross Sections from the RECOIL Data Base, Internal Note RPD/NDS/43 (1991)

3. Lawrence R. Greenwood and Robert K.Smither, SPECTER: Neutron damage calculations for materials irradiations, Report ANL/FPP/TM-197 (1985).

4. S. Selvi and M.M. Ramanadhan, Calculation of Total Damage Cross sections using SPECTER code, Internal Note RPD/NDS/46 (1992).

Preparation of Neutron Gamma Coupled Cross-section Set from ENDF/B-IV Using NJOY Nuclear Data Processing Code

S.Selvi and V.Gopalakrishnan

Reactor Physics Division, IGCAR, Kalpakkam 603 102

A neutron gamma coupled cross section library NEUGAM in 100 neutron energy groups and 21 gamma energy groups was prepared from the basic evaluated nuclear data file ENDF/B-IV using the 1985 version of the Nuclear Data Processing Code NJOY/1/. Anisotropic scattering upto the 5th Legendre order (P5) has been included. DLC-99, the basic library for the photon interaction data, was used for including gamma transport and transfer cross sections. At present 20 materials of interest to reactor sheilding studies at IGCAR have been included in the library NEUGAM. A descriptive note/2/, detailing the options, procedures and the modules of NJOY used for the preparation of NEUGAM was written. Testing of the library NEUGAM is under way. The following are the nuclides included in NEUGAM with their ENDF/B-IV MAT numbers given in brackets:

H(1269), He(1270), B-10(1273), B-11(1160), C(1274), N(1275), O(1276), Na-23(1156), Cr(1191), Fe(1192), Ni (1190), Mn(1197), Co(1199), U-236(1163), U-238(1262), Pu-238(1050), Pu-239(1264), Pu-240(1265), Pu-241(1266), Pu-242(1161).

1. R.L. Mc Farlane and D.W. Muir, The NJOY Nuclear Data Processing System, Vol.1, User's Manual (1982).

2. S.Selvi and V.Gopalakrishnan, Preparation of Neutron Gamma Coupled Cross-section Sets from ENDF/B-IV Using NJOY Nuclear Data Processing Code, Internal Note RPD/NDS/47 (1992).

Published by : M. R. Balakrishnan Head, Library & Information Services Division
Bhabha Atomic Research Centre Bombay 400 085